1. Point-by-point response and relevant changes performed in the manuscript

In this section we inserted a point-by-point response to the Referees together with all relevant changes performed in the manuscript. To facilitate the review, we copied the Referees´ comments below in black and inserted our comments in green. The modifications performed to the manuscript are shown in italic green in quotes.

1.1 Responses to Referee #1

Campos et al., significantly improved the manuscript from the first draft and I appreciate the effort put into the answer to previous comments. Please find below a few comments that should be taken into account before publication.

We thank Referee #1 for the positive review of our manuscript.

1) The new figure 5 is very nice, and the similarity between d13C GeoB6212-1 and atm. pCO2 is striking. This also raises the issue of the interpretation given by the authors: D13C decreases in phase with pCO2 decrease, contrarily to the hypothesis given.

Please note that some 3-dimensional numerical experiments of an AMOC shut-down have been performed with prognostic oceanic and atmospheric d13C. For example, in Menviel et al., 2015, you can see that both the Bern3D and LOVECLIM suggest that NADW shutdown leads to a surface d13C decrease on the Brazilian margin even without enhanced Southern Ocean upwelling. An AMOC shutdown without enhanced Southern Ocean upwelling leads to a small pCO2 decrease (Menviel et al., 2014).

Comment #1 - There is indeed a delay between the minima in our $\delta^{13}C$ records and the maxima in the Siple Dome CO_{2atm} record (Ahn and Brook, 2014). We clearly recognize these offsets in our manuscript (page 8, lines 11-14) and attribute them to uncertainties in the respective age models. It is noteworthy that Ahn and Brook (2014) show the best resolved CO_{2atm} record for HS3 and HS2, and that record shows an increase in CO_{2atm} during HS3 and HS2 (as is highlighted by red arrows in the original publication - please see Fig. 1c from Ahn and Brook (2014)).

2) Abstract and P11, L20-22: With the currently proposed hypothesis (AMOC shutdown leads to enhanced SO upwelling, which decreases SO d13C, releases low d13C into the atmosphere and induce surface d13C decrease on the Brazilian margin), I don't see how the d13C records presented here add evidence to the fact that atmospheric CO2 increase during HS2 and HS3 could have originated from the ocean. Terrestrial carbon release would also increase pCO2, decrease d13CO2 and thus oceanic d13C.

Comment #2 - We agree that based on our data alone we cannot exclude the role of terrestrial carbon release as a potential source for the increase in CO_{2atm}. However, the two primary mechanisms (i.e., (i) AMOC–induced strengthening of Southern Ocean deep water ventilation, and (ii) AMOC–induced weakening of the biological pump) invoked in our manuscript to explain the $\delta^{13}C$ decreases in our records are both related to the oceanic release of CO_2 to the atmosphere. The full rationale for both mechanisms is

described in sections 5.1 and 5.2 of our manuscript, and is supported by previously published records and model experiments. To prevent from misleading the reader, we changed the sentence in the Abstract, as follows (a similar cautionary formulation was also used in the other sentence mentioned by Referee #1):

Page 1, lines 19-20: we added "*Together with other lines of evidence*".

3) In several part of the paper, the authors suggest that similar mechanisms/teleconnctions were at play during all Heinrich stadials (HS2, HS3 often compared to HS1). I understand the rationale, but this is not necessarily true, particularly in the case of HS1, which occurred during the deglaciation … For example, they assume that d13CO2 decreased during HS2 and HS3. It is quite possible, but not yet firmly shown. The very nice d13CO2 record from E'ggleston et al., 2016, unfortunately cannot give that information. They note on p14: "Note that while Heinrich event 2 may also have left a small imprint in our δ13C(atm) record, an unambiguous signal of the weaker Heinrich event 3 cannot be discerned. However, the low resolution in the δ13C(atm) record at that time precludes a final conclusion."

Comment#3 - We agree that changes in $\delta^{13}CO_{2atm}$ for HS3 are still inconclusive because of the lack of the necessary temporal resolution in the available records, despite the evidence from model experiments (Schmittner and Galbraith, 2008; Schmittner and Lund, 2015). Thus, we no longer mention that HS3 was accompanied by a decrease in $\delta^{13}CO_{2atm}$.

Page 2, line 6: we added "*at least for some HS*".

Page 9, line 28: we removed "*HS3 and*".

4) P7, L.26-28: Bauska et al., 2016 present a high-resolution high-quality atmospheric d13CO2 of the last deglaciation, but the modeling experiments performed are extremely idealized and performed with a simple box model. Please note that the impact of changes in southern hemispheric westerlies and/or changes in Antarctic Bottom Water formation on oceanic and atmospheric d13C has been explored using 3-dimensional ocean models including OGCM (e.g. Tschumi et al., 2011; Menviel et al., 2015).

Comment#4 - Agreed. We inserted the references mentioned by Referee #1.

Page 7, line 27: we added "*Model experiments (Tschumi et al., 2011; Menviel et al., 2015*".

1.2 Responses to Referee #2

Overall the authors have addressed most of the major issues raised by the reviewers and the manuscript is close to ready for publication. However, there remain several points that still require attention:

We thank Referee #2 for the positive review of our manuscript.

Page 6, Line 12: Air sea gas exchange very likely played a role in creating the surface ocean d13C anomalies. For example, a large fraction of the modeled decrease in d13C in subtropical gyre locations is due to exchange with a d13C depleted atmosphere (see Figure 6A in Schmittner and Lund, 2015).

Comment #1 - We agree that air-sea gas exchange may have played a role on setting the δ^{13}C anomalies in our records and section 5.3 of our manuscript is entirely devoted to this topic. (Please note that we found no allusion for this topic on the page/lines mentioned by Referee #2).

Page 2, Line 10: While the surface ocean d13C anomalies require a global-scale driver, perhaps via the Southern Ocean, the high resolution intermediate depth records compiled by Hertzberg et al. (2016) show that d13C increased during HS1, which is inconsistent with transport of light carbon by AAIW.

Comment #2 - Indeed, intermediate waters in the western South Atlantic showed an increase in δ^{13}C during HS1, and we clearly mention it in our manuscript (page 9, lines 3-6), citing Tessin and Lund (2013), Lund et al. (2015), Curry and Oppo (2005), and Hertzberg et al. (2016). Moreover, in section 5.1 (more specifically on page 7, lines 29-32, and page 8, lines 1-4) of our manuscript, we suggest that the low δ^{13}C signal could have been transferred to SACW at its region of formation, via SAMW and, to some extent, via AAIW (but, in this case, only up to the Brazil/Malvinas Confluence). (Please note that we found no allusion for this topic on the page/lines mentioned by Referee #2).

Page 2, Line 20: Note that temperature change is not required... an isotopically light surface ocean will cause the atmosphere to be lighter (assuming constant gas exchange rates), with the temperature or wind-driven gas exchange effects acting to modify the isotopic offset between the surface ocean and atmosphere.

Comment #3 - Agreed. An accumulation of ^{13}C–depleted CO_2 in the upper water column will produce a reduction in $\delta^{13}CO_{2atm}$ via air–sea gas exchange. The temperature effect will act as an additional modifier promoting changes in $\delta^{13}CO_{2atm}$.

Page 2, line 19: we removed "*be outgassed to*".

Page 2, line 19: we added "*via air–sea gas exchange*".

Page 2, lines 19-21: we removed "*Since isotopic fractionation between reservoirs is temperature–dependent the air-sea gas exchange during HS1 could have additionally modified $\delta^{13}CO_{2atm}$ (Lynch-Stieglitz et al., 1995).*".

Page 4, Line 6: A minor detail, but air-sea exchange influences d13C of DIC, which then may be incorporated into the foraminiferal shell, with modification by vital effects.

Comment #4 - Agreed. All factors mentioned in page 4, line 6, i.e., calcification temperature, carbonate ion concentration, symbiont activity and air–sea gas exchange can

be incorporated into foraminiferal shell with modification by vital effects. We have changed this passage accordingly.

Page 4, line 7: we added "*with modification by vital effects*".

Page 4, Line 27: What is the interpretation of the sand lenses? Are they turbidites? If so, is there any evidence of anomalous stable isotope results or sedimentation rates above and below the sand layers?

Comment #5 - The sand lenses could indeed be turbidites and to avoid bias in the interpretation of our results we did not sampled these intervals. Additionally, the δ^{13}C and sedimentation rate were not anomalous near these intervals.

Page 5, Line 3-7: Did the authors use mixed planktonic or individual species for the radiocarbon dates? If mixed, were they surface mixed layer or thermocline bugs, or both? What is the basis for assuming the 400 year surface water reservoir age? Is this because surface mixed layer bugs were used for 14C analysis? What is the assumed reservoir age error for the age calibration?

Comment #6 - Table 1 of our manuscript shows in which depths we used individual species, i.e., *G. ruber* (3 radiocarbon ages) and which ones required the use of mixed planktonic foraminifera (11 radiocarbon ages). For these 11 radiocarbon ages we were forced to pool together both mixed layer and thermocline species.

Page 5, lines 2-3: we added: "(*mixed layer and thermocline species)*".

Since we have used a terrestrial calibration curve within the software Bacon 2.2, i.e. IntCal13 (Reimer et al., 2013), it was necessary to apply a correction for reservoir age. This is expressed in the statement (page 5, lines 5-7) "All radiocarbon ages were calibrated with the calibration curve IntCal13 (Reimer et al., 2013) with the software Bacon 2.2 (Blaauw and Christen, 2011). A marine reservoir correction of 400 years was applied with associated error of 100 years (Bard, 1988).".

We chose not to apply a larger reservoir correction than the one suggested for the mixed layer between 40°N and 40°S by Bard (1988) for the samples also containing thermocline species of planktonic foraminifera because the proportion of mixed layer and thermocline species was not determined. However, the 100 yr uncertainty of the reservoir age definitely accommodates any plausible reservoir correction (Franke et al., 2008).

Regarding the reservoir age error, we used an error of 100 yr and added this information to the manuscript.

Page 5, line 7: we added "*with associated error of 100 years*".

Page 6, Line 16: There are two clear negative d13C anomalies during HS2 but the pattern is murkier prior to HS2. While there is a small anomaly at the end of HS3, there is a much larger negative excursion between HS3 and HS2 that doesn't fit the assumed pattern of low d13C during Heinrich stadial events. The authors need to acknowledge this

inconsistency and briefly discuss what may explain the large negative anomaly between HS3 and HS2.

Comment #7 - We agree that the "w-structure" in the δ^{13}C records fit well into HS2, but only partially within HS3. We assume that this is due to age model uncertainties and briefly discussed it in the manuscript.

Page 6, lines 16-17: we added: "*event HS2 and, although the slight offset that is attributed to age model uncertainties, also with*".

Page 7, Line 20: While it is true that the d13C of CDW should decrease with weakening of NADW, there are several additional factors that will influence the d13C tracer field of the ocean interior, related to changes in both preformed and remineralized d13C. For example, the model results of Schmittner and Lund (2015) suggest that remineralization plays the primary role in setting d13C in below 500m water depth in the South Atlantic, Indian, and Pacific Oceans following shutdown of the AMOC (see Figures 5 and 6, Schmittner and Lund, 2015).

Comment #8 - Agreed. In the manuscript, we address these two mechanisms that could account for the decreases observed in our δ^{13}C records, i.e., the role of the Southern Ocean deep water ventilation (section 5.1), and the role of the biological pump (section 5.2). Section 5.2 specifically deals with the topic raised by Referee #2, i.e., preformed and remineralized δ^{13}C in the interior ocean.

Page 7, Line 24: Please qualify that the large Southern Ocean upwelling response occurs only in models with low resolution. Higher resolution models show only minor upwelling sensitivity to large changes in prescribed wind stress in the Southern Ocean, mainly due to eddy compensation (e.g. Farneti and Delworth, Journal of Physical Oceanography, v. 40, 2010).

Comment #9 - Agreed.

Page 7, lines 23-24: we added "*models of low resolution suggest that*".

Page 8, Line 7: This is somewhat selective presentation of evidence... as mentioned above, four separate intermediate depth sites show higher d13C during HS1, which is inconsistent with transport of isotopically light carbon via mode and intermediate waters (Hertzberg et al., 2016).

Comment #10 - Agreed. To prevent misleading the reader, we deleted this sentence.

Page 8, lines 4-7: we removed "*Hendry et al. (2012) describe higher seawater concentrations of Si(OH)4 through silicon isotope composition of sponge spicules (benthic organisms) at intermediate water depths (1048 m water depths) of the western South Atlantic (ca. 27° S) close to our core site during abrupt millennial–scale climate change events, suggesting that the preformed signal from the Southern Ocean could indeed reach subtropical latitudes in the South Atlantic.*".

Page 9, Line 20, Line 23: The d13C of DIC in the surface ocean IS affected by air-sea gas exchange and this would have also been the case during HS events, the question is to what extent. While it is true that the surface ocean rarely reaches equilibrium with the atmosphere, this does not mean the surface ocean doesn't respond to atmospheric variation, especially places like subtropical gyres where there is greater time for equilibration with the atmosphere.

Comment #11 - Agreed.

Page 9, lines 20-21: we added: "*(especially in subtropical gyres, because the longer water residence time in these regions)*".

Page 10, Line 3: Please include best estimate of how much temperature may have affected surface ocean d13C (assuming full equilibration with atmosphere, so it would be a maximum effect).

Comment #12 - The statements mentioned by Referee #2, i.e., "If temperature was the dominant driver, unrealistic changes between 5 and 13 °C would be required to explain the full amplitudes of the δ^{13}C variations.", is not related to the estimates of how much the temperature may have affected surface ocean δ^{13}C, but what should be the range of temperature increase to explain the range of decrease observed in our δ^{13}C records. If our δ^{13}C decreases ranged around 0.5-1.3 ‰, thus the range of increase in temperature required should be around 5-13 ºC, considering a reduction of 0.1 ‰ per °C (Broecker and Maier-Reimer, 1992). However, no high temporal resolution sea surface temperature record is available for HS3 and HS2 in the area of interest of the South Atlantic. Still, nearby records (Barker et al., 2009; Chiessi et al., 2015) show values not larger than 3 ºC for HS1, that showed a notably stronger sea surface temperature anomaly if compared to HS3 and HS2.

Page 10, Line 9: The relationship between sedimentation rate and d13C is inconsistent. While low d13C at the beginning of HS2 corresponds to high sedimentation rate, the even more negative d13C anomaly in mid-HS2 occurs during a relative peak in sedimentation. Also, there is no clear changes in sed. rate during HS3, which should be the case is southward ITCZ migration and greater riverine input of terrigenous material were the main control on sediment accumulation at the core site. To make a convincing case would require multiple cores to constrain sediment discharge from the Plata River basin. Any individual core could represent accumulation related to bottom currents or dynamic sediment accumulation along the margin.

Comment #13 - We agree that the second HS2 peak in sedimentation rate and the respective planktonic δ^{13}C anomaly are not perfectly aligned in time. However, this apparent offset can be exclusively due to: (i) the occurrence of ^{14}C plateaus during HS (e.g., Sarnthein et al., 2007; Franke et al., 2008); and/or (ii) the discretized way our age model was produced in relation to the "continuous" δ^{13}C measurements. Thus, despite of the apparent high temporal resolution showed by the sedimentation rate record of Figure 5i, the information used to produce that curve are the discretized radiocarbon ages.

Choosing ages at slightly different depths may have aligned both records for the second HS2 peak.

Regarding HS3, to the lack of a positive anomaly in sedimentation rates at our core site could be related to the relatively high sea–level during HS3 if compared to the prevailing sea level during HS2 and HS1 (Waelbroeck et al., 2002). The relatively high sea level may have dampened a more significant anomaly in sedimentation rates by shifting the main depocenter towards the continental shelf (e.g., Lantzsch et al., 2014).

To prevent misleading the reader, we added the following sentence to the text.

Page 10, lines 29-31: we added "*However, other factors like shifts in bottom currents and sea level could have also produced the observed changes in sedimentation rates. Detailed age models and more cores from the Rio Grande Cone are necessary to elucidate the main factors controlling the sedimentation rates in that region.*".

Additionally, we emphasized that the "w-structure" is only present in $\delta^{13}C$ for HS3.

Page 10, line 28: we added "*(in this case, only for $\delta^{13}C$)*".

While it is helpful that the authors now include d18O data in the supplemental information, there is no mention of the records here in the discussion. Interestingly, it looks like there is a long-term minimum in d18O at the beginning of HS2, which may be consistent with greater fresh water input to the core site.

Comment #14 - We have not deepened the discussion on the $\delta^{18}O$ records because we believe that: (i) these records do not present clear trends across HS3 and HS2; and (ii) high temporal resolution temperature records from specific depths would be necessary to allow a comprehensive interpretation. Additionally, we mentioned in page 10, line 4 that the $\delta^{18}O$ records are available in the supplementary material.

References

Ahn, J. and Brook, E. J.: Siple Dome ice reveals two modes of millennial CO_2 change during the last ice age, Nature, 5, doi:10.1038/ncomms4723, 2014.

Bard, E.: Correction of accelerator mass spectrometry ^{14}C ages measured in planktonic foraminifera: paleoceanographic implications, Paleoceanography, 3, 635-645, doi:10.1029/PA003i006p00635, 1988.

Barker, S., Diz, P., Vautravers, M. J., Pike, J., Knorr, G., Hall, I. R., and Broecker, W. S.: Interhemispheric Atlantic seesaw response during the last deglaciation, Nature, 457, 1097-1102, doi:10.1038/nature07770, 2009.

Blaauw, M. and Christen, A. J.: Flexible Paleoclimate Age-Depth Models Using an Autoregressive Gamma Process, Bayesian Analysis, 6, 457-474, doi:10.1214/11-BA618, 2011.

Broecker, W. S. and E. Maier-Reimer: The influence of air and sea exchange on the carbon isotope distribution in the sea, Global Biogeochem Cy, 6 (3), 315-320, doi: 10.1029/92GB01672, 1992.

Chiessi, C. M., Mulitza, S., Groeneveld, J., Silva, J. B., Campos, M. C., and Gurgel, M. H. C.: Variability of the Brazil Current during the late Holocene, Palaeogeogr Palaeocl, 415, 28-36, 2014.Chiessi, C. M., Mulitza, S., Mollenhauer, G., Silva, J. B., Groeneveld, J., and Prange, M.: Thermal evolution of the western South Atlantic and the adjacent continent during Termination 1, Clim Past, 11, 915-929, doi:10.5194/cp-11-915-2015, 2015.

Curry, W. B. and Oppo, D. W.: Glacial water mass geometry and the distribution of $\delta^{13}C$ of ΣCO_2 in the western Atlantic Ocean, Paleoceanography, 20, PA1017, doi:10.1029/2004PA001021, 2005.

Franke, J., Paul, A., and Schulz, M.: Modeling variations of marine reservoir ages during the last 45,000 years, Clim Past, 4, 125-136, doi:10.5194/cp-4-125-2008, 2008.

Hendry, K. R., Robinson, L. F., Meredith, M. P., Mulitza, S., Chiessi, C. M., and Arz, H.: Abrupt changes in high-latitude nutrient supply to the Atlantic during the last glacial cycle, Geology, 40, 123-126, doi:10.1130/G32779.1, 2012.

Hertzberg, J. E., Lund, D. C., Schmittner, A., and Skrivanek, A. L.: Evidence for a Biological Pump Driver of Atmospheric CO_2 Rise during Heinrich Stadial 1, Geophys Res Lett, 43, doi:10.1002/2016GL070723, 2016.

Lantzsch, H., Hanebuth, T. J. J., Chiessi, C. M., Schwenk, T., and Violante, R. A.: The high-supply, current-dominated continental margin of southeastern South America during the late Quaternary, Quaternary Res, 81, 339-354, doi:10.1016/j.yqres.2014.01.003, 2014.

Lund, D. C., Tessin, A. C., Hoffman, J. L., and Schmittner, A.: Southwest Atlantic water mass evolution during the last deglaciation, Paleoceanography, 10.1002/2014PA002657, 2015.

Lynch-Stieglitz, J., Stocker, T. F., Broecker, W. S., and Fairbanks, R. G.: The influence of air-sea exchange on the isotopic composition of oceanic carbon: Observations and modeling, Global Biogeochem Cy, 9 (4), 653-665, 1995.

Menviel, L., Mouchet, A., Meissner, K. J., Joos, F., and England, M. H.: Impact of oceanic circulation changes on atmospheric $\delta^{13}CO_2$, Global Biogeochem. Cycles, 29, 1944–1961, doi:10.1002/2015GB005207, 2015.

Reimer, P. J., Bard, E., Bayliss, A., Beck, J. W., Blackwell, P. G., Ramsey, C. B., Buck, C. E., Cheng, H., Edwards, R. L., Friedrich, M., Grootes, P. M., Guilderson, T. P., Haflidason, H., Hajdas, I., Hatte, C., Heaton, T. J., Hoffmann, D. L., Hogg, A. G., Hughen, K. A., Kaiser, K. F., Kromer, B., Manning, S. W., Niu, M., Reimer, R. W., Richards, D. A., Scott, E. M., Southon, J. R., Staff, R. A., Turney, C. S. M., and van der Plicht, J.: IntCal13 and Marine13 radiocarbon age calibration curves 0-50,000 years cal BP, Radiocarbon, 55, 1869-1887, doi:10.2458/azu_js_rc.55.16947, 2013.

Sarnthein, M., Grootes, P. M., Kennett, J. P., and Nadeau, M.-J.: [14]C reservoir ages show deglacial changes in ocean currents and carbon cycle. In: Ocean Circulation: Mechanisms and Impacts - Past and Future Changes of Meridional Overturning (eds A. Schmittner, J. C. H. Chiang and S. R. Hemming), American Geophysical Union, Washington, D. C. doi: 10.1029/173GM13, 2007.

Schmittner, A., and Galbraith, E. D.: Glacial greenhouse-gas fluctuations controlled by ocean circulation changes, Nature, 456, doi:10.1038/nature07531, 2008.

Schmittner, A., and Lund, D. C.: Early deglacial Atlantic overturning decline and its role in atmospheric CO_2 rise inferred from carbon isotopes ($\delta^{13}C$), Clim Past, 11, 135–152, doi:10.5194/cp-11-135-2015, 2015.

Tessin, A. C., and Lund, D. C.: Isotopically depleted carbon in the mid-depth South Atlantic during the last deglaciation, Paleoceanography, 28, 296–306, 2013.

Tschumi, T., Joos, F., Gehlen, M., and Heinze, C.: Deep ocean ventilation, carbon isotopes, marine sedimentation and the deglacial CO_2 rise, Clim Past, 7, 771–800, doi:10.5194/cp-7-771-2011, 2011.

Waelbroeck, C. Labeyriea, L., Michel, E., Duplessy, J. C., McManusc, J. F., Lambeck, K., Balbon, E., and Labracherie, M.: Sea-level and deep water temperature changes derived from benthic foraminifera isotopic records. Quaternary Science Reviews, 21, 1-3, 295-305, 2002.

2. Marked up version of the manuscript

In this section we inserted the marked up revised version of the manuscript. The changes performed to the manuscript are marked up in red.

$\delta^{13}C$ decreases in the upper western South Atlantic during Heinrich Stadials 3 and 2

Marília C. Campos[1], Cristiano M. Chiessi[1], Ines Voigt[2], Alberto R. Piola[3,4], Henning Kuhnert[2], Stefan Mulitza[2]

[1]School of Arts, Sciences and Humanities, University of São Paulo, São Paulo, 03828-000, Brazil
[2]MARUM – Center for Marine Environmental Sciences, University of Bremen, Bremen, 28359, Germany
[3]Servicio de Hidrografia Naval (SHN), Buenos Aires, C1270ABV, Argentina
[4]Dept. Ciencias de la Atmósfera y los Océanos, FCEN, Universidad de Buenos Aires, C1428 EHA, and Instituto Franco–Argentino sobre Estudios de Clima y sus Impactos, CNRS/CONICET, C1428EGA, Argentina

Correspondence to: Marília C. Campos (marilia.carvalho.campos@usp.br)

Abstract. Abrupt millennial–scale climate change events of the last deglaciation (i.e., Heinrich Stadial 1 and the Younger Dryas) were accompanied by marked increases in atmospheric CO_2 (CO_{2atm}) and decreases of its stable carbon isotopic ratios ($\delta^{13}C$), i.e., $\delta^{13}CO_{2atm}$, presumably due to outgassing from the ocean. However, information on the preceding Heinrich Stadials during the last glacial period is scarce. Here we present $\delta^{13}C$ records from two species of planktonic foraminifera from the western South Atlantic that reveal major decreases (up to 1‰) during Heinrich Stadials 3 and 2. These $\delta^{13}C$ decreases are most likely related to millennial–scale periods of weakening of the Atlantic meridional overturning circulation and the consequent increase (decrease) in CO_{2atm} ($\delta^{13}CO_{2atm}$). We hypothesise two mechanisms that could account for the decreases observed in our records, namely strengthening of Southern Ocean deep water ventilation and weakening of the biological pump. Additionally, we suggest that air–sea gas exchange could have contributed to the observed $\delta^{13}C$ decreases. Together with other lines of evidence, oOur data are consistent with the hypothesis that the CO_2 added to the atmosphere during abrupt millennial–scale climate change events of the last glacial period also originated in the ocean and reached the atmosphere by outgassing. The temporal evolution of $\delta^{13}C$ during Heinrich Stadials 3 and 2 in our records is characterized by two relative minima separated by a relative maximum. This "w–structure" is also found in North Atlantic and South American records, further suggesting that such structure is a pervasive feature of Heinrich Stadial 2 and, possibly, also Heinrich Stadial 3.

Keywords: Planktonic Foraminifera. Stable Carbon Isotopes. Heinrich Stadials. Atlantic Meridional Overturning Circulation.

1 Introduction

Heinrich Stadials (HS) are abrupt millennial–scale climate change events marked by an anti-phase interhemispheric temperature pattern which is usually termed the bipolar seesaw (Broecker, 1998). One widely accepted mechanism for the bipolar seesaw is related to changes in the strength of the Atlantic meridional overturning circulation (AMOC), likely caused by fresh water input into high latitudes of the North Atlantic (Mix et al., 1986; Crowley, 1992; Stocker, 1998). During HS, a

weak AMOC occurred simultaneously with cooling in the high latitudes of the surface North Atlantic (Sachs and Lehman, 1999; Bard et al., 2000), warming of the surface South Atlantic (Barker et al., 2009; Chiessi et al., 2015), a southward migration of the Intertropical Convergence Zone (ITCZ) (Arz et al., 1998; Deplazes et al., 2013), strengthening of the South American monsoon system (SAMS) (Cruz et al., 2006; Kanner et al., 2012), and an increase in atmospheric CO_2 (CO_{2atm}) (Ahn and

5   Brook, 2008; Ahn and Brook, 2014). This increase in CO_{2atm} was accompanied by a decrease of its stable carbon isotopic composition ($\delta^{13}CO_{2atm}$), at least for some HS (Eggleston et al., 2016). It has been suggested that the origin of the CO_{2atm} rise and the associated $\delta^{13}CO_{2atm}$ decrease was ocean–sourced (Schmittner and Galbraith, 2008; Anderson et al., 2009; Denton et al., 2010; Mariotti et al., 2016; Eggleston et al., 2016; Hertzberg et al., 2016). The occurrence of stable carbon isotope ($\delta^{13}C$) minima during HS1 (last deglaciation) in planktonic foraminiferal records from the Indo–Pacific Ocean, Southern Ocean, and

10   South Atlantic Ocean (Oppo and Fairbanks, 1989; Ninnemann and Charles, 1997; Mulitza et al., 1999; Spero and Lea, 2002) suggests that the signal originated from the ocean region most directly connected to all major oceanic basins, i.e., the Southern Ocean (Ninnemann and Charles, 1997). Under a weak AMOC, wind–driven upwelling of the Circumpolar Deep Water (CDW) in the Southern Ocean would become stronger, reducing the stratification of the Southern Ocean, and enhancing outgassing of low–$\delta^{13}C$ CO_2 to the atmosphere (Anderson et al., 2009; Denton et al., 2010; Tschumi et al., 2011; Bauska et al. 2016).

15   However, model experiments (e.g., Schmittner and Galbraith, 2008; Schmittner and Lund, 2015) and records from different ocean basins (e.g., Tessin and Lund, 2013; Lund et al., 2015; Curry and Oppo, 2005; Hertzberg et al., 2016) suggest that the increase in CO_{2atm} and decrease in $\delta^{13}CO_{2atm}$ during HS1 are instead related to the weakening of the global oceanic biological pump and the consequent accumulation of ^{13}C–depleted CO_2 in the upper water column. Such anomalously low–$\delta^{13}CO_2$ would then reach ~~be outgassed to~~ the atmosphere via air–sea gas exchange. ~~Since isotopic fractionation between reservoirs is~~

20   ~~temperature–dependent the air–sea gas exchange during HS1 could have additionally modified $\delta^{13}CO_{2atm}$ (Lynch–Stieglitz et al., 1995).~~

The reduction of the upper water column $\delta^{13}C$ caused by one or both of the mechanisms described above may be a common feature of other HS as well but, so far, planktonic foraminiferal $\delta^{13}C$ records corroborating this assumption often only cover the abrupt millennial–scale climate change events of the last deglaciation (i.e., HS1 and the Younger Dryas) while high

25   temporal resolution information on the HS of the last glacial period is still scarce (Oppo and Fairbanks, 1989; Ninnemann and Charles, 1997; Spero and Lea, 2002; Hertzberg et al., 2016). Here we investigate this issue for HS3 and HS2 using planktonic foraminiferal (*Globigerinoides ruber* white (*G. ruber* w) and *Globorotalia inflata* (*G. inflata*)) $\delta^{13}C$ data from a high temporal resolution marine sediment core (GeoB6212-1), collected near 32° S off south–eastern South America (SESA). Our data suggest that HS3 and HS2 were also marked by significant $\delta^{13}C$ decreases in the upper water column.

2 Regional setting

The upper water column of the study area is dominated by the southward flowing Brazil Current (BC) that forms the western branch of the South Atlantic subtropical gyre. The BC is one of the weakest western boundary currents in the world ocean (Peterson and Stramma, 1991) carrying warm, saline and nutrient–depleted subtropical waters southward (Olson et al., 1988). The BC originates near 10-15° S from the bifurcation of the Southern South Equatorial Current as it approaches the western slope of the Brazil Basin (Stramma et al., 1990; Peterson and Stramma, 1991). Around 38° S the BC encounters the northward flowing Malvinas Current (MC), where the opposing flows turn south–east and flow offshore, the so-called Brazil/Malvinas Confluence. The Brazil/Malvinas Confluence is characterized by intense mesoscale variability. After collision and considerable mixing the warm–salty BC fractions flow eastward as the South Atlantic Current (Olson et al., 1988; Peterson and Stramma, 1991), while the majority of the cold fresh MC waters veer southeastward to rejoin the Antarctic Circumpolar Current.

In the study area, the BC transports Tropical Water (TW), South Atlantic Central Water (SACW) and Antarctic Intermediate Water (AAIW). TW occupies the mixed layer, i.e., the upper ca. 100 m of the water column, with a mean temperature of 20 °C and mean salinity of 36 psu (Tsuchiya et al., 1994). TW originates in the tropics-subtropics transition region by subduction, creating a subsurface salinity maximum capping the central waters (Mémery et al., 2000; Tomczak and Godfrey, 2003) (Fig. 1).

SACW occupies the permanent thermocline from ca. 100 to 500 m water depth. Its temperature ranges from 6 to 20 °C and its salinity spans from 34.6 to 36 psu (Mémery et al., 2000). Two types of SACW have been identified (Stramma et al., 2003). The low–density type of SACW which is mainly found in the South Atlantic subtropical gyre is formed by subduction of a low–density type of Subantarctic Mode Water (SAMW) along the southern edge of the gyre (Stramma and England, 1999). The denser variety of SACW originates in the South Indian Ocean and is brought into the South Atlantic by the Agulhas Current (Sprintall and Tomczak, 1993) (Fig. 1).

Just below the permanent thermocline, AAIW occupies the water column from ca. 500 to 1200 m water depth (Stramma and England, 1999). AAIW is characterized as a cold and low salinity water mass (Piola and Georgi, 1982; Tomczak and Godfrey, 2003). Around the southern tip of South America, AAIW originates by subduction of cold and fresh Antarctic Surface Water across the Antarctic Polar Front, and by contribution of a dense type of SAMW that originates from deep winter convection in the Subantarctic Zone (Molinelli, 1981; Naveira Garabato et al., 2009). AAIW is advected eastward through the Drake Passage by the Antarctic Circumpolar Current and turns northwards with the MC into the South Atlantic (Piola and Gordon, 1989). Since AAIW circulation follows the anticyclonic flow of the subtropical gyre the majority of the northward flow at mid-latitude occurs in the eastern basin (McCartney, 1977; Stramma and England, 1999; Tomczak and Godfrey, 2003). However, intense mixing in the Brazil/Malvinas Confluence also leads to direct northward flow in the western South Atlantic that can, to some extent, influence the dissolved inorganic carbon $\delta^{13}C$ ($\delta^{13}C_{DIC}$) in the formation region of SACW (e.g., Piola and Georgi, 1982) (Fig. 1 and 2).

In the modern South Atlantic, the distribution of $\delta^{13}C_{DIC}$ allows the identification of its major water masses. TW and SACW show high $\delta^{13}C_{DIC}$ values of ca. 2‰. AAIW presents $\delta^{13}C_{DIC}$ values of ca. 0.7‰. NADW derives from the North Atlantic and shows $\delta^{13}C_{DIC}$ values of ca. 1‰. In the southwest South Atlantic NADW is sandwiched between Upper and Lower CDW which present $\delta^{13}C_{DIC}$ values of ca. 0.4‰ (Kroopnick, 1985). Since planktonic foraminiferal $\delta^{13}C$ reflects the $\delta^{13}C_{DIC}$ of the

5 ambient seawater, we use it as a proxy for the past oceanic carbon system (Mulitza et al., 1999; Spero, 1992). However, other factors such as calcification temperature, carbonate ion concentration, symbiont activity and air–sea gas exchange may also influence planktonic foraminiferal $\delta^{13}C$ with modification by vital effects (Lynch-Stieglitz et al., 1995; Spero and Lea, 1996, Spero et al., 1997; Bemis et al., 2000).

Changes in upper ocean properties and circulation patterns are also closely associated with changes in the atmospheric

10 circulation. Positive sea surface temperature (SST) anomalies in the western South Atlantic, likely associated to changes in the strength of the AMOC (Knight et al., 2005), have been correlated with positive anomalies in the strength of the SAMS and, consequently, with the increase of precipitation over SESA (Chaves and Nobre, 2004). The SAMS and its main components – the ITCZ, the South Atlantic Convergence Zone (SACZ), and the South American Low Level Jet (SALLJ) – are the main atmospheric drivers of the hydroclimate of tropical and subtropical SESA to the east of the Andes (Garreaud et al., 2009). The

15 ITCZ is a global convective belt in the equatorial region, and the SACZ is an elongate NW-SE convective belt that originates in the Amazon Basin and extends southeastward above the northern portion of SESA and the adjacent subtropical South Atlantic. The SALLJ is a NW-SE humidity flux from the west Amazon Basin to the subtropical region of SESA (Zhou and Lau, 1998; Carvalho et al., 2004). This southward water vapour flux is a crucial source of precipitation to the Plata River drainage basin (Berbery and Barros, 2002), which is a source of continental borne sediments to our core site.

20 **3 Materials and methods**

3.1 Marine sediment core

We investigated sediment core GeoB6212-1 (32.41° S, 50.06° W, 1010 m water depth, 790 cm core length) (Schulz et al., 2001) collected from the continental slope off SESA where the upper water column is under the influence of the BC, and thus the TW and SACW (Fig. 1). This gravity core was raised at the Rio Grande Cone, a major sedimentary feature in the western

25 Argentine Basin. As our study focuses in HS3 and HS2, we analysed the section from the bottom of the core (768 cm core depth; ca. 323 cal ka BP) up to 290 cm core depth (ca. 20 cal ka BP). Visual core inspection provided evidence for the presence of sand lenses at 330 and 368 cm core depth (Schulz et al., 2001; Wefer et al., 2001). Therefore we did not sample these depths. The section of interest of GeoB6212-1 was sampled every 2.5 cm with syringes of 10 cm^3. All samples were wet sieved, oven– dried at 50 °C and the fraction larger than 150 μm was stored in glass vials for subsequent analyses.

3.2 Age model

The age model of core GeoB6212-1 is based on 14 AMS radiocarbon ages from planktonic foraminifera (mixed layer and thermocline species) (Table 1, Fig. 3). For each sample, we hand–picked under a binocular microscope around 10 mg of planktonic foraminifera shells from the sediment fraction larger than 150 μm. Samples were analysed at the Poznan Radiocarbon Laboratory, Poland, and at the Beta Analytic Radiocarbon Dating Laboratory, USA (Table 1). All radiocarbon ages were calibrated with the calibration curve IntCal13 (Reimer et al., 2013) with the software Bacon 2.2 (Blaauw and Christen, 2011). A marine reservoir correction of 400 years was applied with associated error of 100 years (Bard, 1988). All ages are reported as calibrated years before present (cal a BP; present is 1950 AD). To construct the age model we used Bayesian statistics in the software Bacon 2.2 (Blaauw and Christen, 2011). With the exception of mem.mean (set to 0.4) and acc.shape (set to 0.5), default parameters were used. Radiocarbon ages were assumed to be t-distributed with 9 degrees of freedom (t.a=9, t.b=10). Mean ages and 95% error margins were estimated from 10,000 downcore age-depth realizations at 0.5 cm resolution (Fig. 3).

3.3 Stable carbon isotope analyses

Around 10 tests of *G. ruber* w *sensu stricto* (Wang, 2000) within the size range 250-350 μm and 8 tests of *G. inflata* non–encrusted with 3 chamber in the final whorl (Groeneveld and Chiessi, 2011) within the size range 315-400 μm were hand–picked under a binocular microscope every 2.5 cm from 290 to 768 cm core depth. While the first species records the conditions at the top of the mixed layer (down to ca. 30 m) (Chiessi et al., 2007; Wang, 2000), the second species records the conditions at the permanent thermocline (ca. 350-400 m) (Groeneveld and Chiessi, 2011), allowing the reconstruction of the $\delta^{13}C$ signal of the TW and the SACW, respectively. The $\delta^{13}C$ analyses were performed on a Finnigan MAT 252 mass spectrometer equipped with an automatic carbonate preparation device at the MARUM – Centre for Marine Environmental Sciences, University of Bremen, Germany. Isotopic results are reported in the usual delta–notation relative to the Vienna Peedee belemnite. Data were calibrated against the house standard (Solnhofen limestone), itself calibrated against the NBS19 standard. The standard deviation of the laboratory standard was lower than 0.05‰ for the measuring period.

4 Results

4.1 Age model and sedimentation rates

Our age model covers the period between 32 and 6 cal ka BP (Table 1, Fig. 3). Sedimentation rates change markedly during this time interval with values ranging from 5 to 91 cm ka^{-1}. Three main peaks in sedimentation rate were identified at ca. 26, 23 and 15 and one minor peak at 11 cal ka BP. The two oldest sedimentation peaks occur within our period of interest (i.e., from ca. 32̶3̶ until 20 cal ka BP) (Fig. 3). The mean temporal resolution of our $\delta^{13}C$ records is ca. 90 yr with values ranging from 28 to 195 yrs.

4.2 Stable carbon isotope values of *G. ruber* and *G. inflata*

The *G. ruber* w δ¹³C record shows two long–term decreases, from ca. 32 to 28.2 cal ka BP with an amplitude of ca. 1‰, and from ca. 26.5 to 24.9 cal ka BP also with an amplitude of ca. 1‰ (Fig. 4a). These two negative long–term trends are separated from each other by an abrupt increase of ca. 1.3‰ ending at ca. 27.2 cal ka BP. Both long–term decreases were interrupted by
5 brief positive excursions, one from 29.3 to 29.1 cal ka BP with an amplitude of ca. 0.7‰ and another from 26.2 to 25.8 cal ka BP with an amplitude of ca. 1‰. After the second long–term decrease, the δ¹³C values of *G. ruber* w varied around 0.7‰. Both long–term negative excursions determine a pattern we refer to as "w–structure".

The *G. inflata* δ¹³C record shows four negative excursions departing from a baseline of ca. 0.8‰ (Fig. 4b). The first occurs from ca. 31.5 to 29.3 cal ka BP with an amplitude of ca. 0.5‰, the second from ca. 28.8 to 28 cal ka BP with the same
10 amplitude, the third from ca. 26.5 to 26.4 cal ka BP with an amplitude of ca. 0.8‰, and the forth from ca. 25.8 to 24.4 cal ka BP with an amplitude of ca. 0.9‰. Also in the δ¹³C record from *G. inflata* two "w–structures" are present and are defined by the previously described negative excursions.

The "w–structures" as well as the δ¹³C minima are synchronous for both species (Fig. 4).

5 Discussion

15 The synchronous "w–structures" present in the δ¹³C records of both planktonic foraminiferal species analysed here occur in coeval with the millennial–scale event HS2 and, although the slight offset that is attributed to age model uncertainties, also with events HS3 and HS2 (Sarnthein et al., 2001; Goni and Harrison, 2010) (Fig. 4). Concomitantly, a weak AMOC was described based on ²³¹Pa/²³⁰Th records from the Bermuda Rise (ODP Site 1063, 33.7° N, 57.6° W) (Lippold et al., 2009) (Fig. 5d). Both events are also marked by pulses of ice-rafted debris (IRD) (MD99-2331, 42.2° N, 9.7° W) (Eynaud et al., 2009)
20 and by decreases in SST (SU8118 and MD952042, 37.5° N, 10.1° W) (Bard, 2000) in the north–eastern North Atlantic (Iberian Margin). The Greenland GISP2 ice core (72.6° N, 38.5° W) shows synchronous increases in Ca^{+2}, indicating changes in atmospheric circulation over Greenland (Mayewski et al., 1997) (Fig. 5a, b, c). It is noteworthy that the four records (i.e., Fig. 5a, b, c, d) mentioned above also show a "w–structure" during HS2, similar to the one shown in our δ¹³C records. The IRD (Eynaud et al., 2009) and Ca^{+2} (Mayewski et al., 1997) records also show a "w–structure" similar to ours during HS3.

25 Based on modern conditions, we expect our core site not to be significantly influenced by changes in the local nutrient content of the upper water column since the region is dominated by the oligotrophic BC, characteristic of western boundary currents, and is far from upwelling cells (Brandini et al., 2000). Thus, it is unlikely that changes in our δ¹³C records are associated with local productive events driven by nutrient–cycle processes (Mulitza et al., 1999).

During HS, we expect warmer temperatures to have occurred in the upper water column of the western South Atlantic (Barker
30 et al. 2009; Chiessi et al. 2015). This would trigger an increase in δ¹³C values of the symbiont–bearing species investigated here if calcification temperature would dominate the δ¹³C signal (Bemis et al., 2000), which is not the case (Fig. 4a).

Additionally, given the lack of regional upper ocean reconstructions for carbonate ion concentration, we assume that increased CO_{2atm} that is frequently associated with HS (Ahn and Brook, 2008; Ahn and Brook, 2014) would have been accompanied by a decrease in sea surface carbonate ion concentration (Broecker and Peng, 1993). This would promote an increase in the $\delta^{13}C_{DIC}$ but our records show a negative $\delta^{13}C$ anomaly (Fig. 4). Furthermore, we analysed a symbiont–bearing and a facultative–symbiont species (i.e., *G. ruber* w and *G. inflata*, respectively) and both records show a similar pattern (Fig. 4) indicating that changes in symbiont activity can also be disregarded as a factor influencing our results (Spero et al., 1997; Bemis et al., 2000). We propose two primary mechanisms to explain our $\delta^{13}C$ decreases: (i) changes in the strength of Southern Ocean deep water ventilation (detailed in section 5.1), and (ii) the weakening of the global oceanic biological pump (detailed in section 5.2). Additionally, air–sea gas exchange may have acted as a secondary factor contributing to our $\delta^{13}C$ decreases (detailed in section 5.3).

5.1 Millennial–scale changes: AMOC–induced strengthening of Southern Ocean deep water ventilation

A negative excursion during HS1 was described in planktonic foraminiferal $\delta^{13}C$ records from the Indo–Pacific Ocean (Spero and Lea, 2002), Southern Ocean (Ninnemann and Charles, 1997), and South Atlantic Ocean (Oppo and Fairbanks, 1989). Ninnemann and Charles (1997) suggested that the source for this signal was the Southern Ocean.

In the Southern Ocean CDW forms from mixing of NADW, Indian Deep Water (IDW) and Pacific Deep Water (PDW) and upwells to the south of the Antarctic Polar Front driven by the prevailing westerly winds (Marshall and Speer, 2012). Therefore, the $\delta^{13}C$ signature of CDW (ca. 0.4‰) (Kroopnick, 1985) lies between that of NADW (ca. 1‰) (Kroopnick, 1985) and IDW/PDW (ca. 0.2 to -0.2‰) (Kroopnick, 1985) (Oppo and Fairbanks, 1987; Charles and Fairbanks, 1992). During periods of weak AMOC the inflow of NADW to the Southern Ocean is reduced (Charles and Fairbanks, 1992), and the $\delta^{13}C$ of CDW should decrease since the latter would have a relatively larger contribution from low–$\delta^{13}C$ IDW and PDW (Spero and Lea, 2002).

Additionally, during periods of reduced AMOC the sub–tropical heat transport towards the north would decrease, leading to rising temperatures in the circum–Antarctic region (EPICA Community Members, 2006). Consequently, models of low resolution suggest that the Southern Hemisphere westerlies would become stronger and shift southward, strengthening CDW upwelling (Toggweiler et al., 2006; Tschumi et al., 2011; Lee et al., 2011; Voigt et al., 2015). Increased upwelling would supply the ocean surface south of the Antarctic Polar Front with $Si(OH)_4$–rich, low–$\delta^{13}C$ waters (Anderson et al., 2009; Hendry et al., 2012). A recent mModel experiments (Tschumi et al., 2011; Menviel et al., 2015; Bauska et al., 2016) corroborates this hypothesis by showing that stronger Southern Ocean upwelling would promote a weakening of the biological pump in the Southern Ocean. Since upwelled CDW is hypothesized to be the dominant source of the upper and intermediate waters that leave the Southern Ocean (i.e., SAMW and AAIW) (Fig. 2), increased upwelling would transfer the low $\delta^{13}C$ signal as well as the positive $Si(OH)_4$ anomaly to those waters (Oppo and Fairbanks, 1989; Ninnemann and Charles, 1997; Spero and Lea, 2002; Anderson et al., 2009; Hendry et al., 2012). Actually, a low–density type of SAMW contributes to SACW that spreads

into the South Atlantic (Stramma and England, 1999). Additionally, AAIW also influences SACW through vigorous eddy mixing at the Brazil/Malvinas Confluence (Piola and Georgi, 1982). These signals would then propagate through the thermocline SACW of the South Atlantic, and be transferred to the mixed layer TW by vertical exchange process (Tomczak and Godfrey, 2003). ~~Hendry et al. (2012) describe higher seawater concentrations of Si(OH)$_4$ through silicon isotope~~
5 ~~composition of sponge spicules (benthic organisms) at intermediate water depths (1048 m water depths) of the western South~~ ~~Atlantic (ca. 27° S) close to our core site during abrupt millennial–scale climate change events, suggesting that the preformed~~ ~~signal from the Southern Ocean could indeed reach subtropical latitudes in the South Atlantic.~~

The reduced stratification of the Southern Ocean and intensification of the upward transport of the remineralized carbon (^{12}C–enriched CO_2) stored for a long period in deep waters (Anderson et al., 2009; Denton et al., 2010; Jaccard et al., 2016; Mariotti
10 et al., 2016) would increase CO_{2atm} (Siple Dome, 81.7° S, 148.8° W) (Ahn and Brook, 2014) (Fig. 5j). Despite the low temporal resolution, Eggleston et al.'s (2016) Antarctic $\delta^{13}CO_{2atm}$ record shows a decrease during HS2. However, the CO_{2atm} peaks occur ca. 1 ka later than the initiation of the δ^{13}C decrease in our records. Spero and Lea (2002) also observed a similar offset between the increase in CO_{2atm} and the decrease in Pacific Ocean planktonic foraminifera δ^{13}C during HS1, and attributed this apparent offset to uncertainties in the age models of their records.
15 Therefore, the negative excursions in our δ^{13}C records could be related to the transfer of a preformed δ^{13}C signal from the subantarctic zone to the western South Atlantic via central and thermocline waters.

5.2 Millennial–scale changes: AMOC–induced weakening of the biological pump

Recent model experiments (e.g. Schmittner, 2005; Schmittner and Galbraith, 2008) have shown that AMOC slowdown events may cause a decrease in the global efficiency of the oceanic biological pump, being an important driver for the oceanic CO_2
20 outgassing within HS1 during the last deglaciation and possibly also during other HS, including HS3 and HS2.
NADW has low preformed nutrient waters because it is formed by nutrient depleted surface waters, where the biological pump has efficiently removed nutrients from surface waters (Marinov et al., 2008). AABW has high preformed nutrient waters because it is formed by nutrient–enriched Southern Ocean surface waters (nutrients have not being efficiently removed from surface waters). However, during weak AMOC two factors may alter the nutrient distribution and the global oceanic biological
25 pump (Schmittner and Galbraith, 2008). First, the reduction in the NADW formation decreases the input of low preformed nutrient (high $\delta^{13}C_{DIC}$) waters to the ocean interior which becomes more dominated by high preformed nutrient (low $\delta^{13}C_{DIC}$) southern component waters (e.g., AABW). Second, the reduction of the Southern Ocean stratification induced by the decrease of salt input via NADW formation promotes the strengthening of the upwelling and subsequent sinking of high preformed nutrient (low $\delta^{13}C_{DIC}$) waters to the ocean interior, thus reducing the capacity of those unutilized nutrients to sequester carbon
30 via the biological pump. The two factors acting in conjunction are thought to be responsible for the simulated weakening of the global efficiency of the biological pump, as well as for the increase in CO_{2atm} and decrease in $\delta^{13}CO_{2atm}$ (Schmittner and Galbraith, 2008; Schmittner and Lund, 2015; Hertzberg et al., 2016).

Schmittner and Lund (2015) show that the modeled weakening of the biological pump, induced by an AMOC slowdown, reduces the ability of the surface ocean to biologically sequester isotopically light organic carbon (^{12}C), producing a decrease in the surface ocean $\delta^{13}C_{DIC}$ and an increase of the intermediate ocean $\delta^{13}C_{DIC}$ (lower remineralization rate). For HS1, planktonic and benthic foraminiferal $\delta^{13}C$ records (Tessin and Lund, 2013; Lund et al., 2015; Curry and Oppo, 2005; Hertzberg

5   et al., 2016) from the western South Atlantic (ca. 27°S) agree with the model output by showing a decrease in $\delta^{13}C$ in the upper water column (SACW) and an increase at intermediate water depths (AAIW). Thus, the weakening of the global oceanic biological pump and consequent negative anomaly of the $\delta^{13}C_{DIC}$ in the upper water column should be captured by the tests of planktonic foraminifera $\delta^{13}C$ during calcification (Spero and Lea, 1996; Bemis et al., 2000). The negative $\delta^{13}C_{DIC}$ during HS3 and HS2 revealed by our planktonic foraminifera provide the first observational evidence supporting the modeling results.

10   Additionally, this mechanism also provides a possible explanation for the larger negative $\delta^{13}C$ anomaly in *G. ruber* w (mixed layer dwelling) relative to the anomaly in *G. inflata* (permanent thermocline dwelling) (Fig. 4).

It is noteworthy that the mechanism described in section 5.1, although based on a different driver for the decrease in $\delta^{13}C$, also suggests that the decreases in $\delta^{13}C$ of planktonic foraminifera from the South Atlantic would be carried by SACW (inherited from its precursor, SAMW) and thus both mechanisms (described in section 5.1 and here) are in this regard not mutually

15   exclusive. However, the mechanism described in the present section goes against the assumption that weakening of the biological pump is related to stronger upwelling in the Southern Ocean, and that the Southern Ocean would be the source of the low $\delta^{13}C$ signal for the South Atlantic (Lund et al., 2015; Hertzberg et al., 2016).

5.3 Millennial–scale changes: the role of air–sea gas exchange

The $\delta^{13}C_{DIC}$ of the surface ocean can also be affected by air–sea gas exchange (Oppo and Fairbanks, 1989; Charles and

20   Fairbanks, 1990; Lynch-Stieglitz et al., 1995). Although this process tends towards isotopic equilibrium (especially in subtropical gyres, because the longer water residence time in these regions), the CO_2 exchange between the ocean and the atmosphere does not lead to equilibrium because CO_2 uptake and emission will still occur in different regions and the movement and replacement of surface waters is faster than required for equilibration (Lynch-Stieglitz et al., 1995). Since the $\delta^{13}CO_{2atm}$ is lighter than $\delta^{13}C_{DIC}$, at areas of ocean CO_{2atm} uptake (i.e., water mass formation regions) air–sea gas exchange has

25   the potential to deplete $\delta^{13}C_{DIC}$ (Lynch-Stieglitz et al., 1995). Additionally, the isotopic fractionation is inversely correlated with temperature.

Therefore, we cannot exclude the possibility that the likely decrease in $\delta^{13}CO_{2atm}$ during AMOC slowdown events (Eggleston et al. 2016) (e.g., HS3 and HS2) could have affected the $\delta^{13}C_{DIC}$ via air–sea gas exchange, especially in regions of water mass formation. The formation region of SACW is an area of ocean CO_2 uptake and may contribute to the $\delta^{13}C$ anomalies observed

30   in our *G. inflata* record (Fig. 4b). Additionally, since the isotopic fractionation during air–sea gas exchange is temperature–dependent the weakening of the AMOC and subsequent warming of the upper subtropical South Atlantic (Barker et al. 2009; Chiessi et al. 2015) could have contributed to the observed $\delta^{13}C$ anomalies both in the *G. ruber* w and in the *G. inflata* records

(Fig. 4). However, the gradient is too small (-0.1‰ $\delta^{13}C$ per °C, Broecker and Maier-Reimer, 1992) to explain the whole changes observed in our records. If temperature was the dominant driver, unrealistic changes between 5 and 13 °C would be required to explain the full amplitudes of the $\delta^{13}C$ variations.

The $\delta^{18}O$ records from *G. ruber* w and *G. inflata* from our core (Supplementary material Figure 1) should partially reflect changes in water temperature (ca. -0.22‰ per 1 °C; e.g., Mulitza et al, 2003), but show no clear trends across HS3 and HS2. While temperature changes might be partially obscured in the foraminiferal $\delta^{18}O$ records by the influence of synchronous changes in seawater-$\delta^{18}O$, as has been hypothesized for the Holocene (Chiessi et al., 2014) and HS1 (Chiessi et al., 2015) in the western Atlantic, we consider it unlikely that temperature changes of the above magnitude would be completely masked.

5.4 Changes in continental climate

Paleoclimate records from South America indicate marked hydrological changes during abrupt millennial–scale climate events (Arz et al., 1998; Peterson et al., 2000; Baker et al., 2001; Cruz et al., 2006; Stríkis et al., 2015). Reconstructed SAMS activity suggests strengthening during HS (Cruz et al., 2006; Kanner et al., 2012; Cheng et al., 2013). Changes in speleothem oxygen isotopic composition from the western Amazon Basin (NAR-C, Cueva del Diamante cave, northern Peru, 5.4° S, 77.3° W) (Cheng et al., 2013) as well as changes on gamma radiation records from the Bolivian Altiplano (Salar de Uyuni, 20.3° S, 67.5° W) (Baker et al., 2001) (Fig. 5f, g) indicate increased precipitation during HS3 and HS2. North of the equator, a reflectance record from the Cariaco Basin (off northern Venezuela, MD03-2621, 10.7° N, 65° W) (Deplazes et al., 2013) suggests decreased precipitation during the same millennial–scale events (Fig. 5e). The opposite precipitation variations at these sites reflects the interhemispheric anti-phased response of tropical precipitation during HS (Wang et al., 2007; Cheng et al., 2013). During HS3 and particularly HS2 the three above mentioned records (Fig. 5e, f, g) show a "w–structure" similar to the one observed in our $\delta^{13}C$ records. Stríkis et al. (2015) reported a similar "w–structure" during HS1 related to two distinct hydrologic phases within HS1.

Periods of intensified SAMS would have strengthened the discharge from the Plata River drainage basin (Chiessi et al., 2009), increasing the delivery of terrigenous sediments to the Rio Grande Cone (Lantzsch et al., 2014), our coring site. Our records present for the first time increased sedimentation rates during a HS off SESA and corroborate the suggestion of Chiessi et al. (2009) during HS2. Furthermore, GeoB6212-1 sedimentation rates also show a "w–structure" during HS2 (Fig. 3), hinting for a sensitive response of the Plata River drainage basin to the increase in activity of the SAMS. The occurrence of a similar "w–structure" in North Atlantic records, in South American records and in our $\delta^{13}C$ and sedimentation rate records gives us confidence that such "w–structure" is indeed an ubiquitous feature of HS2, and possibly also HS3 (in this case, only for $\delta^{13}C$). However, other factors like shifts in bottom currents and sea level could have also produced the observed changes in sedimentation rates. Detailed age models and more cores from the Rio Grande Cone are necessary to elucidate the main factors controlling the sedimentation rates in that region.

The increased continental runoff that led to increased delivery of terrigenous sediments to our core site could have also enhanced the nutrient availability and the local primary productivity, affecting our planktonic foraminiferal $\delta^{13}C$ records. Some aspects of the regional response to HS1 are useful to evaluate this possibility. During HS1, ice volume corrected seawater– $\delta^{18}O$ from the upper water column of our core site indicates an increase in salinity (Chiessi et al., 2015). Thus, despite of the

5 increased terrigenous discharge, it seems that the upper water column of our core site was not affected by an increase in freshwater discharge from the Plata River during HS1. Since the precipitation anomaly of HS1 was stronger than that of HS3 and HS2 in the Plata River drainage basin (Wang et al., 2007), it is unlikely that weaker precipitation anomalies of HS3 and HS2 would have impacted the upper water column of our core site more intensely than during HS1. This suggests that changes in the discharge of the Plata River drainage basin at millennial–scale are not a relevant driver of our $\delta^{13}C$ decreases, and that

10 the buoyant low salinity waters were advected elsewhere by winds, while terrigenous sediments were already too deep to be influenced by the wind.

6 Conclusions

Our mixed layer and permanent thermocline $\delta^{13}C$ records from the western South Atlantic show in-phase millennial–scale decreases of up to 1‰ during the HS3 and HS2. We hypothesize that the low $\delta^{13}C$ signal may be related to two millennial–

15 scale mechanisms. (i) Changes in the Southern Ocean deep water ventilation. A weak AMOC during HS3 and HS2 would produce stronger Southern Ocean upwelling that in turn, would supply the surface of the Southern Ocean with more low–$\delta^{13}C$ waters as well as promote increased outgassing of this old and low–$\delta^{13}C$ respired CO_2. The low–$\delta^{13}C$ waters at the surface of the Southern Ocean would be subducted into the central and thermocline waters and transferred equatorward via the South Atlantic subtropical gyre circulation and southward along the western boundary towards our core site. (ii) Weakening of the

20 global oceanic biological pump. A weak AMOC during HS3 and HS2 would promote an accumulation of ^{13}C–depleted CO_2 in the upper water column of the South Atlantic. This accumulation would result in a negative anomaly of the $\delta^{13}C_{DIC}$ (as well as of the $\delta^{13}CO_{2atm}$) that in turn would be captured by the tests of planktonic foraminifera at our core site. We further suggest that changes in air–sea gas exchange could have contributed to the decreases in $\delta^{13}C$ via both mechanisms. Together with other lines of evidence, our data are consistent with the hypothesis that the CO_2 added to the atmosphere during abrupt millennial–

25 scale climate change events of the last glacial period originated in the ocean and reached the atmosphere by outgassing. Moreover, the occurrence of a similar "w–structure" during HS2 (and possibly HS3) in North Atlantic and South American records as well as in our planktonic foraminiferal $\delta^{13}C$ and sedimentation rate records gives us confidence that such "w–structure" is a pervasive feature that characterizes HS2 (and possibly HS3).

Data availability

30 The data reported here will be archived in Pangaea (www.pangaea.de).

Acknowledgements

References

Ahn, J. and Brook, E. J.: Atmospheric CO_2 and climate on millennial time scales during the last glacial period, Science, 322, 83-85, doi:10.1126/science.1160832, 2008.

Ahn, J. and Brook, E. J.: Siple Dome ice reveals two modes of millennial CO_2 change during the last ice age, Nature Communications, 5, doi:10.1038/ncomms4723, 2014.

Andersen, K. K., Svensson, A., Johnsen, S. J., Rasmussen, S. O., Bigler, M., Rothlisberger, R., Ruth, U., Siggaard-Andersen, M.-L., Steffensen, J. P., Dahl-Jensen, D., Vinther, B. M., and Clausen, H.B.: The Greenland Ice Core Chronology 2005, 15-42 ka. Part 1: constructing the time scale, Quaternary Sci Rev, 25, 3246-3257, doi:10.1016/j.quascirev.2006.08.002, 2006.

Anderson, R. F., Ali, S., Bradtmiller, L. I., Nielsen, S. H. H., Fleisher, M. Q., Anderson, B. E., and Burckle, L. H.: Wind-Driven Upwelling in the Southern Ocean and the Deglacial Rise in Atmospheric CO_2, Science, 323, 1443-1448, doi:10.1126/science.1167441, 2009.

Arz, H. W., Pätzold, J., and Wefer, G.: Correlated millennial-scale changes in surface hydrography and terrigenous sediment yield inferred from last-glacial marine deposits off northeastern Brazil, Quaternary Res, 50, 157-166, doi:10.1006/qres.1998.1992, 1998.

Baker, P. A., Rigsby, C. A., Seltzer, G. O., Fritz, S. C., Lowenstein, T. K., Bacher, N. P., and Veliz, C.: Tropical climate changes at millennial and orbital timescales on the Bolivian Altiplano, Nature, 409, 698-701, doi:10.1038/35055524, 2001.

Bard, E.: Correction of accelerator mass spectrometry ^{14}C ages measured in planktonic foraminifera: paleoceanographic implications, Paleoceanography, 3, 635-645, doi:10.1029/PA003i006p00635, 1988.

Bard, E., Rostek, F., Turon, J. L., and Gendreau, S.: Hydrological impact of Heinrich events in the subtropical northeast Atlantic, Science, 289, 1321-1324, doi:10.1126/science.289.5483.1321, 2000.

Barker, S., Diz, P., Vautravers, M. J., Pike, J., Knorr, G., Hall, I. R., and Broecker, W. S.: Interhemispheric Atlantic seesaw response during the last deglaciation, Nature, 457, 1097-1102, doi:10.1038/nature07770, 2009.

Bauska, T., K., Baggenstos, D., Brook, E. J., Mix, A. C., Marcott, S. A., Petrenko, V. V., Schaefer, H., Severinghaus, J. P., and Lee, J. E.: Carbon isotopes characterize rapid changes in atmospheric carbon dioxide during the last deglaciation, P Natl Acad Sci USA, 113, 13, 3465–3470, doi:10.1073/pnas.1513868113, 2016.

Bemis, B. E., Spero, H. J., Lea, D. W., and Bijma, J.: Temperature influence on the carbon isotopic composition of *Globigerina bulloides* and *Orbulina universa* (planktonic foraminifera), Mar Micropaleontol, 38, 213–228, doi:10.1016/S0377-8398(00)00006-2, 2000.

Berbery, E. H. and Barros, V. R.: The hydrologic cycle of the La Plata basin in South America, J Hydrometeorol, 3, 630-645, doi:10.1175/1525-7541(2002)003<0630:THCOTL>2.0.CO;2, 2002.

Blaauw, M. and Christen, A. J.: Flexible Paleoclimate Age-Depth Models Using an Autoregressive Gamma Process, Bayesian Analysis, 6, 457-474, doi:10.1214/11-BA618, 2011.

Brandini, F. P., Boltovskoy, D., Piola, A., Kocmur, S., Röttgers, R., Cesar Abreu, P., and Mendes Lopes, R.: Multiannual trends in fronts and distribution of nutrients and chlorophyll in the southwestern Atlantic (30–62° S), Deep-Sea Res Pt I, 47, 1015-1033, doi:10.1016/S0967-0637(99)00075-8, 2000.

Broecker, W. S.: Paleocean circulation during the last deglaciation: A bipolar seesaw? Paleoceanography, 13, 119-121, doi:10.1029/97PA03707, 1998.

Broecker, W. S. and Peng, T.-H.: What caused the glacial to interglacial CO2 change? In The Global Carbon Cycle (ed. Heimann, M.) 95–115, Springer, Berlin, 1993.

Broecker, W. S. and E. Maier-Reimer: The influence of air and sea exchange on the carbon isotope distribution in the sea, Global Biogeochem Cy, 6 (3), 315-320, doi: 10.1029/92GB01672, 1992.

Carvalho, L. M. V., Jones, C., and Liebmann, B.: The South Atlantic convergence zone: Intensity, form, persistence, and relationships with intraseasonal to interannual activity and extreme rainfall, J Climate, 17, 88-109, doi:http://dx.doi.org/10.1175/1520-0442(2004)017<0088:TSACZI>2.0.CO;2, 2004.

Charles, C. D. and Fairbanks, R. G.: Evidence from Southern-Ocean sediments for the effect of North-Atlantic Deep-Water flux on climate, Nature, 355, 416-419, doi:10.1038/355416a0, 1992.

Charles, C. D., and Fairbanks, R. G.: Glacial to interglacial changed in the isotopic gradients of Southern Ocean surface water, in Geological History of the Polar Oceans: Arctic Versus Antarctic, edited by U. Bleil and J. Thiede, pp. 519-538, Kluwer Academic, Norwell, Mass., 1990.

Chaves, R. R. and Nobre, P.: Interactions between sea surface temperature over the South Atlantic Ocean and the South Atlantic Convergence Zone, Geophys Res Lett, 31, doi:10.1029/2003GL018647, 2004.

Cheng, H., Sinha, A., Cruz, F. W., Wang, X., Edwards, R. L. A., d'Horta, F. M., Ribas, C. C., Vuille, M., Stott, L. D., and Auler, A. S.: Climate change patterns in Amazonia and biodiversity, Nature Communications, 4, doi:10.1038/ncomms2415, 2013.

Chiessi, C. M., Ulrich, S., Mulitza, S., Paetzold, J., and Wefer, G.: Signature of the Brazil-Malvinas Confluence (Argentine Basin) in the isotopic composition of planktonic foraminifera from surface sediments, Mar Micropaleontol, 64, 52-66, doi:10.1016/j.marmicro.2007.02.002, 2007.

Chiessi, C. M., Mulitza, S., Groeneveld, J., Silva, J. B., Campos, M. C., and Gurgel, M. H. C.: Variability of the Brazil Current during the late Holocene, Palaeogeogr, Palaeoclim, Palaeoecol, 415, 28-36, doi:10.1016/j.palaeo.2013.12.005, 2014.

Chiessi, C. M., Mulitza, S., Paetzold, J., Wefer, G., and Marengo, J. A.: Possible impact of the Atlantic Multidecadal Oscillation on the South American summer monsoon, Geophys Res Lett, 36, L21707, doi:10.1029/2009GL039914, 2009.

Chiessi, C. M., Mulitza, S., Mollenhauer, G., Silva, J. B., Groeneveld, J., and Prange, M.: Thermal evolution of the western South Atlantic and the adjacent continent during Termination 1, Clim Past, 11, 915-929, doi:10.5194/cp-11-915-2015, 2015.

Crowley, T. J.: North Atlantic Deep Water cools the Southern Hemisphere, Paleoceanography, 7, 489-497, doi:10.1029/92PA01058, 1992.

Cruz, F. W., Jr., Burns, S. J., Karmann, I., Sharp, W. D., and Vuille, M.: Reconstruction of regional atmospheric circulation features during the late Pleistocene in subtropical Brazil from oxygen isotope composition of speleothems, Earth Planet Sc Lett, 248, 495-507, doi:10.1016/j.epsl.2006.06.019, 2006.

Curry, W. B. and Oppo, D. W.: Glacial water mass geometry and the distribution of $\delta^{13}C$ of ΣCO_2 in the western Atlantic Ocean, Paleoceanography, 20, PA1017, doi:10.1029/2004PA001021, 2005.

Denton, G. H., Anderson, R. F., Toggweiler, J. R., Edwards, R. L., Schaefer, J. M., and Putnam, A. E.: The Last Glacial Termination, Science, 328, 1652-1656, doi:10.1126/science.1184119, 2010.

Deplazes, G., Lueckge, A., Peterson, L. C., Timmermann, A., Hamann, Y., Hughen, K. A., Roehl, U., Laj, C., Cane, M. A., Sigman, D. M., and Haug, G. H.: Links between tropical rainfall and North Atlantic climate during the last glacial period, Nat Geosci, 6, 213-217, doi:10.1038/ngeo1712, 2013.

Eggleston, S., Schmitt, J., Bereiter, B., Schneider, R., and Fischer, H.: Evolution of the stable carbon isotope composition of atmospheric CO2 over the last glacial cycle, Paleoceanography, doi:10.1002/2015PA002874, 2016.

EPICA Community Members: One-to-one coupling of glacial climate variability in Greenland and Antarctica, Nature, 444, 195-198, doi:10.1038/nature05301, 2006.

Eynaud, F., de Abreu, L., Voelker, A., Schoenfeld, J., Salgueiro, E., Turon, J.-L., Penaud, A., Toucanne, S., Naughton, F., Goni, M. F. S., Malaize, B., and Cacho, I.: Position of the Polar Front along the western Iberian margin during key cold episodes of the last 45 ka, Geochem Geophy Geosy, 10, doi:10.1029/2009GC002398, 2009.

Garreaud, R. D., Vuille, M., Compagnucci, R., and Marengo, J.: Present-day South American climate, Palaeogeogr Palaeocl, 281, 180-195, doi:10.1016/j.palaeo.2007.10.032, 2009.

Goni, M. F. S. and Harrison, S. P.: Millennial-scale climate variability and vegetation changes during the Last Glacial: Concepts and terminology Introduction, Quaternary Sci Rev, 29, 2823-2827, doi:10.1016/j.quascirev.2009.11.014, 2010.

Groeneveld, J. and Chiessi, C. M.: Mg/Ca of *Globorotalia inflata* as a recorder of permanent thermocline temperatures in the South Atlantic, Paleoceanography, 26, doi:10.1029/2010pa001940, 2011.

Guilderson, T. P. and Pak, D. K.: Salinity proxies $\delta^{18}O$. In: Encyclopedia of Quaternary: Paleoceanography, Physical and Chemical proxies. Elsevier: Amsterdam, p. 1766-1775, 2007.

Hendry, K. R., Robinson, L. F., Meredith, M. P., Mulitza, S., Chiessi, C. M., and Arz, H.: Abrupt changes in high-latitude nutrient supply to the Atlantic during the last glacial cycle, Geology, 40, 123-126, doi:10.1130/G32779.1, 2012.

5 Hertzberg, J. E., Lund, D. C., Schmittner, A., and Skrivanek, A. L.: Evidence for a Biological Pump Driver of Atmospheric CO2 Rise during Heinrich Stadial 1, Geophys Res Lett, 43, doi:10.1002/2016GL070723, 2016.

Jaccard, S. L., Galbraith, E. D., Martínez-García, A., and Anderson, R. F.: Covariation of deep Southern Ocean oxygenation and atmospheric CO_2 through the last ice age, Nature, 530, 207-210, doi:10.1038/nature16514, 2016.

Kanner, L. C., Burns, S. J., Cheng, H., and Edwards, R. L.: High-Latitude Forcing of the South American Summer Monsoon

10 During the Last Glacial, Science, 335, 570-573, doi:10.1126/science.1213397, 2012.

Knight, J. R., Allan, R. J., Folland, C. K., Vellinga, M., and Mann, M. E.: A signature of persistent natural thermohaline circulation cycles in observed climate, Geophys Res Lett, 32, L20708, doi:10.1029/2005GL024233, 2005.

Kroopnick, P. M.: The distribution of C-13 of sigma-CO_2 in the world oceans, Deep-Sea Res, 32, 57-84, doi:10.1016/0198-0149(85)90017-2, 1985.

15 Lantzsch, H., Hanebuth, T. J. J., Chiessi, C. M., Schwenk, T., and Violante, R. A.: The high-supply, current-dominated continental margin of southeastern South America during the late Quaternary, Quaternary Res, 81, 339-354, doi:10.1016/j.yqres.2014.01.003, 2014.

Lee, S.-Y., Chiang, J. C. H., Matsumoto, K., and Tokos, K. S.: Southern Ocean wind response to North Atlantic cooling and the rise in atmospheric CO2: Modeling perspective and paleoceanographic implications, Paleoceanography, 26, PA1214,

20 doi:10.1029/2010PA002004, 2011.

Lippold, J., Gruetzner, J., Winter, D., Lahaye, Y., Mangini, A., and Christl, M.: Does sedimentary $^{231}Pa/^{230}Th$ from the Bermuda Rise monitor past Atlantic Meridional Overturning Circulation? Geophys Res Lett, 36, doi:10.1029/2009GL038068, 2009.

Locarnini, R. A., Mishonov, A. V., Antonov, J. I., Boyer, T. P., Garcia, H. E., Baranova, O. K., Zweng, M. M., Paver, C. R.,

25 Reagan, J. R., Johnson, D. R., Hamilton, M., and Seidov, D.: World Ocean Atlas 2013, Volume 1: Temperature, in: Levitus, S., Mishonov, A. (Eds.). NOAA Atlas NESDIS, p. 40, 2013.

Lund, D. C., Tessin, A. C., Hoffman, J. L., and Schmittner, A.: Southwest Atlantic water mass evolution during the last deglaciation, Paleoceanography, 10.1002/2014PA002657, 2015.

Lynch-Stieglitz, J., Stocker, T. F., Broecker, W. S., and Fairbanks, R. G.: The influence of air-sea exchange on the isotopic

30 composition of oceanic carbon: Observations and modeling, Global Biogeochem Cy, 9 (4), 653-665, 1995.

Marinov, I., Gnanadesikan, A., Sarmiento, J. L., Toggweiler, J. R., Follows, M., and Mignone, B. K.: Impact of oceanic circulation on biological carbon storage in the ocean and atmospheric pCO2. Global Biogeochem Cy 22, GB3007, doi:10.1029/2007GB002958, 2008.

Mariotti, V., Paillard, D., Bopp, L., Roche, D. M., and Bouttes, N.: A coupled model for carbon and radiocarbon evolution during the last deglaciation, Geophys Res Lett, 43, doi:10.1002/2015GL067489, 2016.

Marshall, J. and Speer, K.: Closure of the meridional overturning circulation through Southern Ocean upwelling, Nat Geosci, 5, 171-180, doi:10.1038/ngeo1391, 2012.

Mayewski, P. A., Meeker, L. D., Twickler, M. S., Whitlow, S., Yang, Q. Z., Lyons, W. B., and Prentice, M.: Major features and forcing of high-latitude northern hemisphere atmospheric circulation using a 110,000-year-long glaciochemical series, J Geophys Res-Oceans, 102, 26345-26366, doi:10.1029/96JC03365, 1997.

McCartney, M. S.: Subantarctic Mode Water, in: Angel, M.V. (Ed.), A Voyage of Discovery. Oxford, 1977.

Mémery, L., Arhan, M., Alvarez-Salgado, X. A., Messias, M. J., Mercier, H., Castro, C. G., and Rios, A. F.: The water masses along the western boundary of the south and equatorial Atlantic, Prog Oceanogr, 47, 69-98, doi:10.1016/S0079-6611(00)00032-X, 2000.

Menviel, L., Mouchet, A., Meissner, K. J., Joos, F., and England, M. H.: Impact of oceanic circulation changes on atmospheric $\delta^{13}CO_2$, Global Biogeochem. Cycles, 29, 1944–1961, doi:10.1002/2015GB005207, 2015.

Mix, A. C., Ruddiman, W. F., and McIntyre, A.: Late Quaternary paleoceanography of the Tropical Atlantic, 1: spatial variability of annual mean sea-surface temperatures, 0-20,000 years BP, Paleoceanography, 1, 43-66, 10.1029/PA001i001p00043, 1986.

Molinelli, E. J.: The Antarctic influence on Antarctic Intermediate Water, J Mar Res, 39, 267-293, 1981.

Mulitza, S., Arz, H., Mücke, S. K., Moos, C., Niebler, H. -S., Pätzold, J., and Segl, M.: The South Atlantic Carbon Isotope Record of Planktic Foraminifera, in: Fischer, G., Wefer, G. (Eds.), Use of Proxies in Paleoceanography: Examples from South Atlantic. Springer-Verlag, Berlin Heidelberg, pp. 427-445, 1999.

Naveira Garabato, A. C. N., Jullion, L., Stevens, D. P., Heywood, K. J., and King, B. A.: Variability of Subantarctic Mode Water and Antarctic Intermediate Water in the Drake Passage during the Late-Twentieth and Early-Twenty-First Centuries, J Climate, 22, 3661-3688, doi:http://dx.doi.org/10.1175/2009JCLI2621.1, 2009.

Ninnemann, U. S. and Charles, C. D.: Regional differences in Quaternary Subantarctic nutrient cycling: Link to intermediate and deep water ventilation, Paleoceanography, 12, 560-567, doi:10.1029/97PA01032, 1997.

Olson, D. B., Podesta, G. P., Evans, R. H., and Brown, O. B.: Temporal variations in the separation of Brazil and Malvinas currents, Deep-Sea Res, 35, 1971-1990, doi:10.1016/0198-0149(88)90120-3, 1988.

Oppo, D. W. and Fairbanks, R. G.: Variability in the deep and intermediate water circulation of the Atlantic-Ocean during the past 25,000 years - Northern-Hemisphere modulation of the Southern-Ocean, Earth Planet Sc Lett, 86, 1-15, doi:10.1016/0012-821X(87)90183-X, 1987.

Oppo, D. W. and Fairbanks, R. G.: Carbon isotope composition of tropical surface water during the past 22,000 years, Paleoceanography, 4, 333-351, doi:10.1029/PA004i004p00333, 1989.

Peterson, L. C., Haug, G. H., Hughen, K. A., and Rohl, U.: Rapid changes in the hydrologic cycle of the tropical Atlantic during the last glacial, Science, 290, 1947-1951, doi:10.1126/science.290.5498.1947, 2000.

Peterson, R. G. and Stramma, L.: Upper-level circulation in the South-Atlantic Ocean, Prog Oceanogr, 26, 1-73, doi:10.1016/0079-6611(91)90006-8, 1991.

Piola, A. R. and Georgi, D. T.: Circumpolar properties of Antarctic Intermediate Water and Sub-antarctic Mode Water, Deep-Sea Res, 29, 687-711, doi:10.1016/0198-0149(82)90002-4, 1982.

Piola, A. R. and Gordon, A. L.: Intermediate waters in the southwest South-Atlantic, Deep-Sea Res, 36, 1-16, doi:10.1016/0198-0149(89)90015-0, 1989.

Rasmussen, S. O., Andersen, K. K., Svensson, A. M., Steffensen, J. P., Vinther, B. M., Clausen, H. B., Siggaard-Andersen, M. L., Johnsen, S. J., Larsen, L. B., Dahl-Jensen, D., Bigler, M., Rothlisberger, R., Fischer, H., Goto-Azuma, K., Hansson, M. E., and Ruth, U.: A new Greenland ice core chronology for the last glacial termination, J Geophys Res-Atmos, 111, D06102, doi:10.1029/2005jd006079, 2006.

Reimer, P. J., Bard, E., Bayliss, A., Beck, J. W., Blackwell, P. G., Ramsey, C. B., Buck, C. E., Cheng, H., Edwards, R. L., Friedrich, M., Grootes, P. M., Guilderson, T. P., Haflidason, H., Hajdas, I., Hatte, C., Heaton, T. J., Hoffmann, D. L., Hogg, A. G., Hughen, K. A., Kaiser, K. F., Kromer, B., Manning, S. W., Niu, M., Reimer, R. W., Richards, D. A., Scott, E. M., Southon, J. R., Staff, R. A., Turney, C. S. M., and van der Plicht, J.: IntCal13 and Marine13 radiocarbon age calibration curves 0-50,000 years cal BP, Radiocarbon, 55, 1869-1887, doi:10.2458/azu_js_rc.55.16947, 2013.

Sachs, J. P. and Lehman, S. J.: Subtropical North Atlantic temperatures 60,000 to 30,000 years ago, Science, 286, 756-759, doi:10.1126/science.286.5440.756, 1999.

Rohling, E. J. and Cooke, E.: Stable oxygen and carbon isotopes in foraminiferal carbonate shells. In: Sen Gupta, B. K.,: Modern Foraminifera. Kluwer Academic Publishers, p. 239-259, 1999.

Sarnthein, M., Stattegger, K., Dreger, D., Erlenkeuser, H., Grootes, P., Haupt, B. J., Jung, S., Kiefer, T., Kuhnt, W., Pflaumann, U., Schafer-Neth, C., Schulz, H., Schulz, M., Seidov, D., Simstich, J., van Kreveld, S., Vogelsang, E., Volker, A., and Weinelt, M.: Fundamental modes and abrupt changes in north Atlantic circulation and climate over the last 60 ky - Concepts, reconstruction and numerical modeling in: The Northern North Atlantic: A Changing Environment, edited by: Schäfer, P., Ritzrau, W., Schlüter, M., and Thiede, J., Springer, Berlin, 365–410, 2001.

Schmittner, A. and Galbraith, E. D.: Glacial greenhouse-gas fluctuations controlled by ocean circulation changes, Nature, 456, doi:10.1038/nature07531, 2008.

Schmittner, A., and Lund, D. C.: Early deglacial Atlantic overturning decline and its role in atmospheric CO2 rise inferred from carbon isotopes (δ^{13}C), Clim Past, 11, 135–152, doi:10.5194/cp-11-135-2015, 2015.

Schneider, T., Bischoff, T., and Haug, G. H.: Migrations and dynamics of the intertropical convergence zone, Nature, 513, 45-53, doi:10.1038/nature13636, 2014.

Schulz, H. D., Ayres Neto, A., Boetius, A., Enneking, K., Fabian, K., Feseker, T., Funk, J., Gorke, M., Heidersdorf, F., Hensen, C., Heuer, V., Hill, H. G., Hinrichs, S., Kasten, S., Klann, M., Lacerda de Souza, C., Martinez Briao, A., Meyer, S., Mulitza, S., Niebler, H.-S., Ochsenhirt, W.-T., Panteleit, B., Pfeifer, K., Schewe, F., Schwenk, T., Senorans, J. L., Siemer, S., Steinmetz,

E., and Wenzhöfer, F.: Report and preliminary results of Meteor Cruise M46/2, Recife (Brazil) – Montevideo (Uruguay), 2 December – 29 December 1999, Fachbereich Geowissenschaften, Universität Bremen, Bremen, 107 pp., 2001.

Spero, H. J. and Lea, D. W.: Experimental determination of stable isotope variability in *Globigerina bulloides*: Implications for paleoceanographic reconstruction, Mar Micropaleontol, 28, 231–246, doi:10.1016/0377-8398(96)00003-5, 1996.

5 Spero, H. J., Bijma, J., Lea, D., and Bemis, B. E.: Effect of seawater carbonate concentration on foraminiferal carbon and oxygen isotopes, Nature, 390, doi:10.1038/37333, 1997.

Spero, H. J.: Do planktic foraminifera accurately record shifts in the carbon isotopic composition of seawater sigma-CO_2? Mar Micropaleontol, 19, 275-285, doi:10.1016/0377-8398(92)90033-G, 1992.

Spero, H. J. and Lea, D. W.: The cause of carbon isotope minimum events on glacial terminations, Science, 296, 522-525,

10 doi:10.1126/science.1069401, 2002.

Sprintall, J. and Tomczak, M.: On the formation of central water and thermocline ventilation in the Southern-Hemisphere, Deep-Sea Res Pt I, 40, 827-848, doi:10.1016/0967-0637(93)90074-D, 1993.

Stocker, T. F.: Climate change - The seesaw effect, Science, 282, 61-62, doi:10.1126/science.282.5386.61, 1998.

Stramma, L. and England, M. H.: On the water masses and mean circulation of the South Atlantic Ocean, J Geophys Res-

15 Oceans, 104, 20863-20883, doi:10.1029/1999JC900139, 1999.

Stramma, L., Ikeda, Y., and Peterson, R. G.: Geostrophic transport in the Brazil Current region north of 20-degrees-S, Deep-Sea Res, 37, 1875-1886, doi:10.1016/0198-0149(90)90083-8, 1990.

Stramma, L., Fischer, J., Brandt, P., and Schott, F.: Circulation, variability and near-equatorial meridional flow in the central tropical Atlantic, Elsev Oceanogr Serie, 68, 1-22, doi:10.1016/S0422-9894(03)80141-1, 2003.

20 Stríkis, N. M., Chiessi, C. M., Cruz, F. W., Vuille, M., Cheng, H., de Souza Barreto, E. A., Mollenhauer, G., Kasten, S., Karmann, I., Edwards, R. L., Pablo Bernal, J., and Sales, H. D. R.: Timing and structure of Mega-SACZ events during Heinrich Stadial 1, Geophys Res Lett, 42, 5477-5484, doi:10.1002/2015GL064048, 2015.

Svensson, A., Andersen, K. K., Bigler, M., Clausen, H. B., Dahl-Jensen, D., Davies, S. M., Johnsen, S. J., Muscheler, R., Parrenin, F., Rasmussen, S. O., Roethlisberger, R., Seierstad, I., Steffensen, J. P., and Vinther, B. M.: A 60 000 year Greenland

25 stratigraphic ice core chronology, Clim Past, 4, 47-57, doi:10.5194/cp-4-47-2008, 2008.

Tessin, A. C. and Lund, D. C.: Isotopically depleted carbon in the mid-depth South Atlantic during the last deglaciation, Paleoceanography, 28, 296–306, 2013.

Toggweiler, J. R., Russell, J. L., and Carson, S. R.: Midlatitude westerlies, atmospheric CO2, and climate change during the ice ages, Paleoceanography, 21, PA2005, doi:10.1029/2005PA001154, 2006.

30 Tomczak, M. and Godfrey, J. S.: Regional Oceanography: An Introduction, 2nd ed. Daya Publishing House, Delhi, 2003.

Tschumi, T., Joos, F., Gehlen, M., and Heinze, C.: Deep ocean ventilation, carbon isotopes, marine sedimentation and the deglacial CO2 rise, Clim Past, 7, 771–800, doi:10.5194/cp-7-771-2011, 2011.

Tsuchiya, M., Talley, L. D., and McCartney, M. S.: Water-mass distributions in the western South-Atlantic - a section from South Georgia Island (54S) northward across the equator, J Mar Res, 52, 55-81, doi:http://dx.doi.org/10.1357/0022240943076759, 1994.

Voigt, I., Chiessi, C. M., Prange, M., Mulitza, S., Groeneveld, J., Varma, V., and Henrich, R.: Holocene shifts of the southern westerlies across the South Atlantic, Paleoceanography, doi:10.1002/2014PA002677, 2015.

Wang, L. J.: Isotopic signals in two morphotypes of *Globigerinoides ruber* (white) from the South China Sea: implications for monsoon climate change during the last glacial cycle, Palaeogeogr Palaeocl, 161, 381-394, doi:10.1016/S0031-0182(00)00094-8, 2000.

Wang, X., Auler, A. S., Edwards, R. L., Cheng, H., Ito, E., Wang, Y., Kong, X., and Solheid, M.: Millennial-scale precipitation changes in southern Brazil over the past 90,000 years, Geophys Res Lett, 34, doi:10.1029/2007GL031149, 2007.

Wefer, G., Adegbie, A. T., Böckel, B., Brauner, R., Büttner, U., Diekamp, V., Dillon, M., Dobeneck, T. v., Donner, B., Eberwein, A., Heinecke-Herzog, M., Kim, J. H., Meier, S., Mollenhauer, G., Olguin, H., Romero, O., Schewe, F., Schlemm, V., Schmieder, F., Schünemann, H., Streng, M., and Volbers, A. N. A.: Report and preliminary results of Meteor Cruise M46/4, Mar del Plata (Argentina) – Salvador da Bahia (Brazil), 10 February – 13 March 2000, With partial results of Meteor Cruise M46/2., Fachbereich Geowissenschaften, Universität Bremen, Bremen, 136 pp., 2001.

Zhou, J. Y. and Lau, K. M.: Does a monsoon climate exist over South America? J Climate, 11, 1020-1040, doi:http://dx.doi.org/10.1175/1520-0442(1998)011<1020:DAMCEO>2.0.CO;2, 1998.

Table 1: Accelerator mass spectrometer radiocarbon dates and calibrated ages used to construct the age model of core GeoB6212-1.

Core depth (cm)	Lab ID	Species	Radiocarbon age ± 1σ error (a BP)	Calibrated ages (cal a BP)
8	Poz-47236*	*G. ruber*	5250 ± 40	5929
33	382580**	*G. ruber*	9440 ± 40	10047
58	Poz-47237*	*G. ruber*	10250 ± 50	11395
113	382581**	Planktonic forams	12870 ± 50	14342
158	Poz-47238*	Planktonic forams	13050 ± 70	15247
253	382582**	Planktonic forams	15750 ± 50	18620
323	382583**	Planktonic forams	17560 ± 60	20748
363	Poz-47239*	Planktonic forams	18610 ± 140	21834
478	382584**	Planktonic forams	19810 ± 70	23537
578	Poz-47240*	Planktonic forams	21750 ± 150	25587
623	382585**	Planktonic forams	22320 ± 80	26184
668	382586**	Planktonic forams	22480 ± 80	26711
717	424077**	Planktonic forams	24190 ± 110	27850
768	382587**	Planktonic forams	29520 ± 160	31966

* Poz: Poznan Radiocarbon Laboratory, Poznan, Poland.
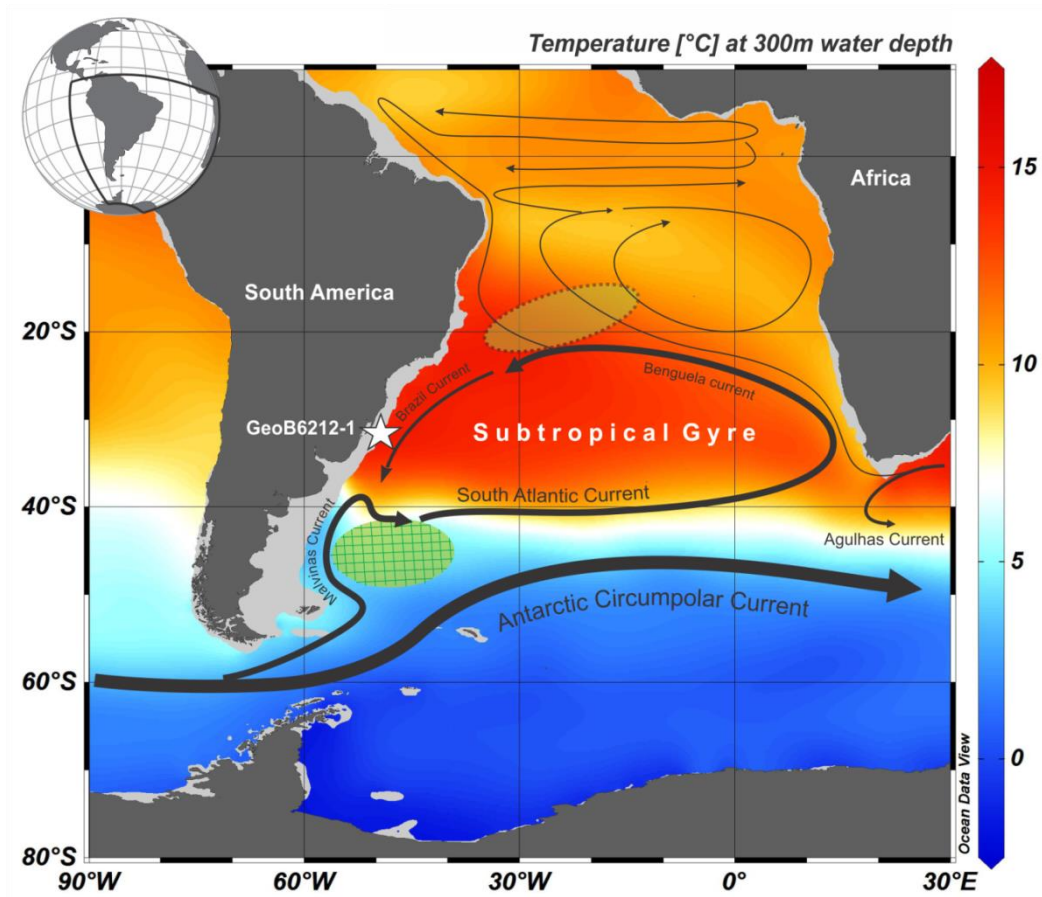** Beta Analytic Radiocarbon Dating Laboratory, Miami, USA.

Figure 1: Schematic representation of the large–scale circulation of South Atlantic Central Water (SACW) (Stramma and England, 1999). The main SACW source region is depicted by the gridded green ellipse, and the main source region of tropical subsurface water (TW) is indicated by the dotted yellow ellipse. Mean annual temperature at 300 m water depth is shown by the colour shading (Locarnini et al., 2013) (http://odv.awi.de).
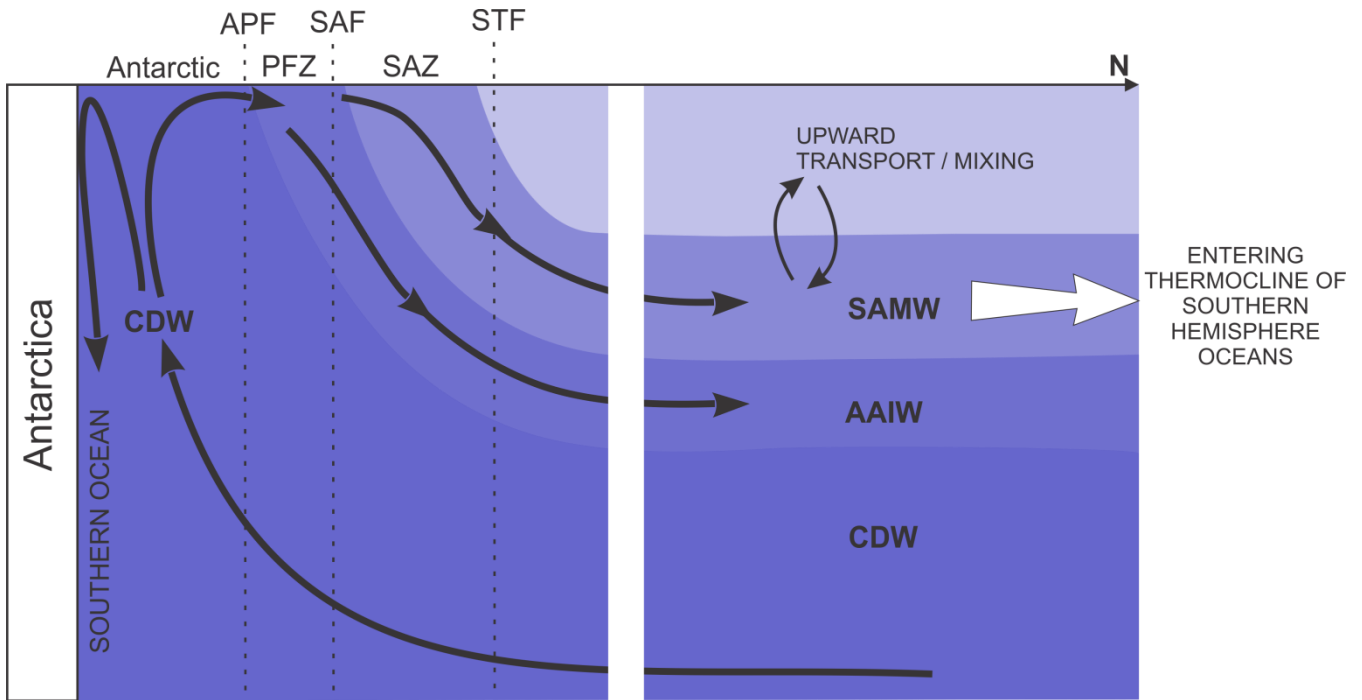
Figure 2: Schematic representation of ventilation and subduction of water masses in the Southern Ocean (modified after Anderson et al., 2009). Wind–driven upwelling south of the latitude of maximum westerlies brings Circumpolar Deep Water (CDW) to the surface and contributes to Antarctic Surface Waters. Antarctic Surface Waters represent the dominant source of the upper and intermediate waters that leave the Southern Ocean. Antarctic Intermediate Water (AAIW) originates by subduction of cold and fresh Antarctic Surface Waters across the Antarctic Polar Front (APF) and enters the South Atlantic mainly via the subtropical gyre. Subantarctic Mode Water (SAMW) originates from deep winter convection north of the Subantarctic Front (SAF). A low–density type of SAMW enters the thermocline of the Southern Hemisphere oceans along the southern edge of the subtropical gyres where it becomes part of central waters and contributes to ventilating the thermocline, while a denser type of SAMW formed in the eastern South Pacific is regarded as a precursor of the AAIW. The Polar Front Zone (PFZ) and Subantarctic Zone (SAZ) are the regions between the APF and SAF, and between the SAF and Subtropical Front (STF), respectively.
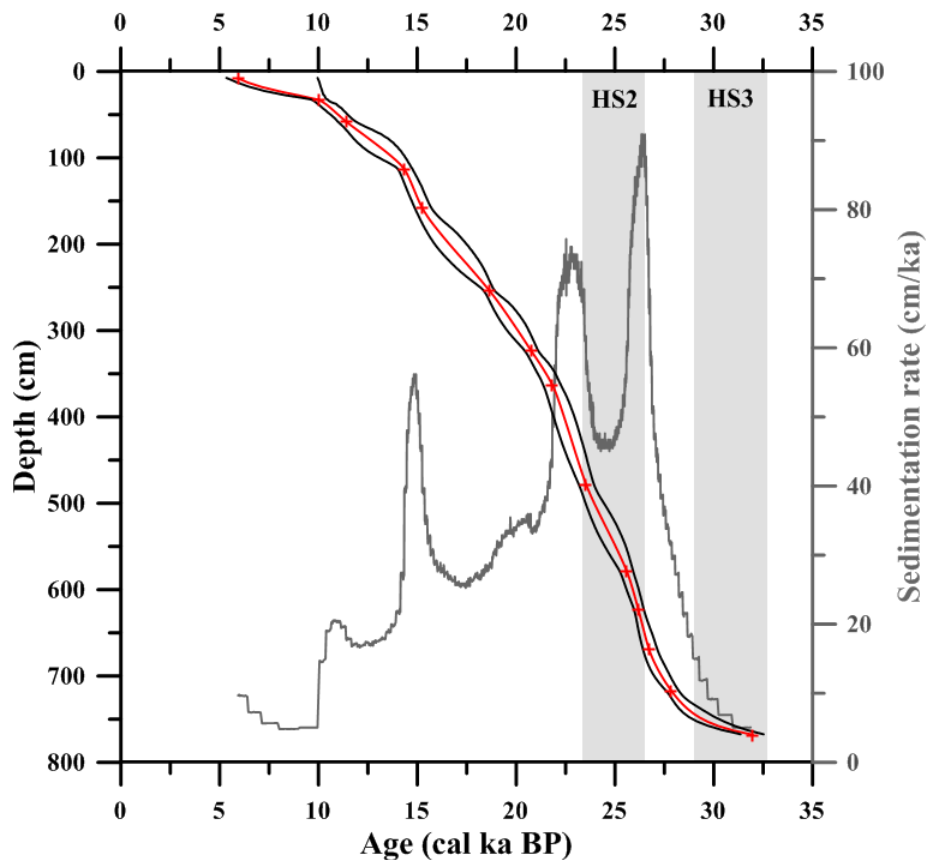
Figure 3: Age model (left hand side y–axis; red line and black enveloping curves) and sedimentation rates (right hand side y–axis; grey line) for marine sediment core GeoB6212-1 produced with the software Bacon 2.2 (Blaauw and Christen, 2011). For the age model, the red symbols show calibrated ages, the red line depicts mean ages and the upper (lower) black line depicts maximum (minimum) ages. Grey vertical bars show abrupt millennial–scale climate change events Heinrich Stadial 3 (HS3) and Heinrich Stadial 2 (HS2) (Goni and Harrison, 2010; Sarnthein et al., 2001).
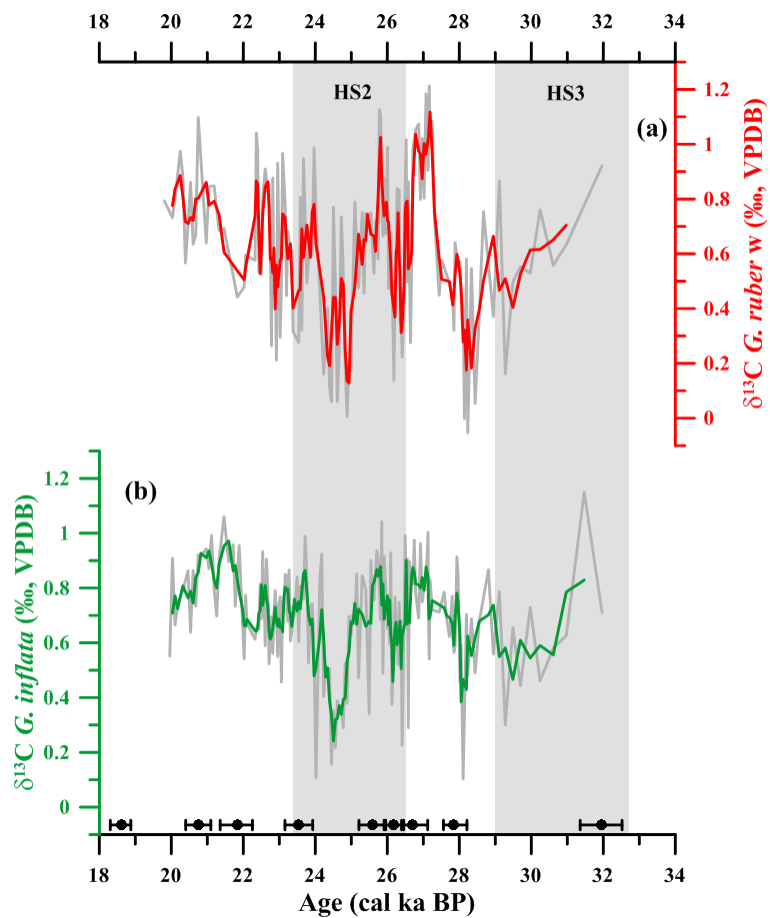
Figure 4: Stable carbon isotopic (δ¹³C) records from sediment core GeoB6212-1. (a) *Globigerinoides ruber* **white (***G. ruber* **w) δ¹³C and (b)** *Globorotalia inflata* **(***G. inflata***) δ¹³C. Red and green lines represent three–point running averages for** *G. ruber* **w and** *G. inflata***, respectively. Black symbols at the bottom of the panel depict calibrated ages. Grey vertical bars show abrupt millennial–scale climate change events Heinrich Stadial 3 (HS3) and Heinrich Stadial 2 (HS2) (Goni and Harrison, 2010; Sarnthein et al., 2001).**
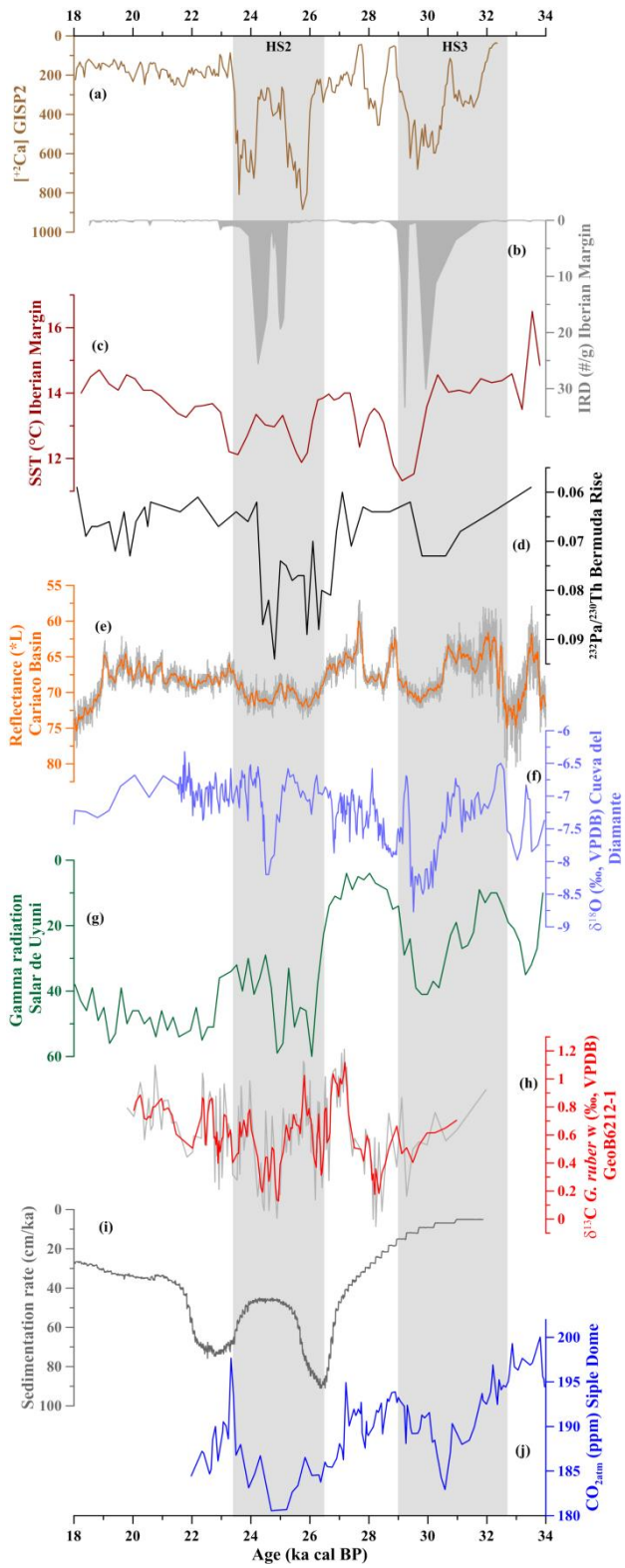
Figure 5: Proxy records from the western South Atlantic, western and eastern North Atlantic and tropical South America spanning Heinrich Stadial 3 (HS3) and Heinrich Stadial 2 (HS2) (Goni and Harrison, 2010; Sarnthein et al., 2001). (a) Changes in atmospheric circulation over Greenland derived from Greenland Ice Sheet Project 2 (GISP2) Ca^{+2} concentration (Mayewski et al., 1997) plotted versus the Greenland Ice Core Chronology 2005 (GICC05) (Andersen et al., 2006; Rasmussen et al., 2006) at 72.6° N, 38.5° W; (b)
5   **Heinrich layers indicated by the presence of ice-rafted debris (IRD) from the Iberian Margin marine sediment core MD99-2331 at 42.2° N, 9.7° W (Eynaud et al., 2009); (c) sea surface temperature (SST) (°C) changes from Iberian Margin marine sediment cores SU8118 and MD952042 at 37.5° N, 10.1° W (Bard, 2000); (d) Atlantic meridional overturning circulation (AMOC) strength derived from Bermuda Rise sedimentary $^{231}Pa/^{230}Th$ ratio – ODP Site 1063 (higher values indicate a reduced AMOC) at 33.7° N, 57.6° W (Lippold et al., 2009); (e) position of the Intertropical Convergence Zone (ITCZ) indicated by reflectance (*L) (higher values indicate**
10   **decreased precipitation) from the Cariaco Basin marine sediment core MD03-2621 at 10.7° N, 65° W (Deplazes et al., 2013) (orange line represents a 399-point running average); (f) strength of western Amazon precipitation indicated by the $\delta^{18}O$ from stalagmite NAR-C collected in the Cueva del Diamante Cave, western Amazon (more negative values indicate increased precipitation) at 5.4° S, 77.3° W (Cheng et al., 2013); (g) presence of paleolakes indicated by the natural gamma radiation from Bolivian Altiplano Salar de Uyuni (higher values indicate increased precipitation) at 20.3° S, 67.5° W (Baker et al., 2001); (h) *Globigerinoides ruber* white (*G.***
15   ***ruber* w) $\delta^{13}C$ from marine sediment core GeoB6212-1 collected in the western South Atlantic at 32.4° S, 50.1° W (red line represents a three–point running average) (this study); (i) sedimentation rates from marine sediment core GeoB6212-1 collected in the western South Atlantic at 32.4° S, 50.1° W (this study); (j) atmospheric CO_2 concentration (ppm) from ice core Siple Dome (Ahn and Brook, 2014) plotted versus the Greenland Ice Core Chronology 2005 (GICC05) (Svensson et al., 2008) at 81.7° S, 148.8° W.**